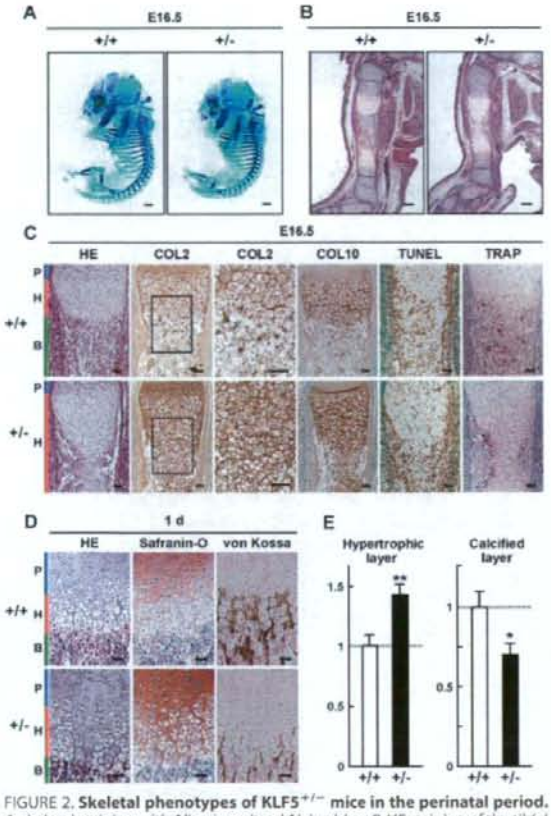

FIGURE 2. **Skeletal phenotypes of KLF5$^{+/-}$ mice in the perinatal period.** *A*, skeletal staining with Alizarin red and Alcian blue; *B*, HE staining of the tibial limbs of wild-type (+/+) and KLF5$^{+/-}$ embryos (E16.5). *Scale bars*, 1 mm and 200 μm, respectively. *C*, HE, COL2, and COL10 immunostainings and TUNEL and TRAP stainings of the tibial limbs of wild-type and KLF5$^{+/-}$ embryos (E16.5). *Inset boxes* in the *left COL2 panels* indicate the regions of the respective *right COL2 panels*. *Blue*, *red*, and *green bars* indicate proliferative (*P*) and hypertrophic (*H*) layers and bone area (*B*), respectively. *Scale bars*, 50 μm. *D*, HE, Safranin-O, and von Kossa stainings of the growth plates in proximal tibias of wild-type and KLF5$^{+/-}$ neonates (1 day). *Scale bars*, 50 μm. *E*, relative lengths of hypertrophic layer (*left*) and calcified layer (*right*) in KLF5$^{+/-}$ growth plate compared with those in wild type (1 day). Data are expressed as means (*bars*) ± S.E. (*error bars*) for 4 mice/group. *, $p < 0.05$; **, $p < 0.01$ *versus* wild type.

TABLE 1

Changes in expression of genes related to matrix degradation by KLF5 overexpression

mRNA levels in OUMS27 cells with adenoviral introduction of KLF5 and the control empty vector were compared by RT2 profiler PCR array (APHS-016; SuperArray Bioscience). For MMP19 and -20 and ADAMTS4, -5, -9, and -15, real time RT-PCR was performed using primer sets shown in the supplemental materials. ND, not detected.

Gene symbol	GenBank™ accession number	Increase
		-fold
MMP1	NM_002421	3.1
MMP2	NM_004530	1.6
MMP3	NM_002422	−1.3
MMP7	NM_002423	−1.4
MMP8	NM_002424	2.1
MMP9	NM_004994	2,143.9
MMP10	NM_002425	−1.1
MMP11	NM_005940	−1.8
MMP12	NM_002426	1.4
MMP13	NM_002427	−2.1
MMP14	NM_004995	2.6
MMP15	NM_002428	3.9
MMP16	NM_005941	−1.6
MMP19	NM_002429	1.6
MMP20	NM_004771	ND
ADAMTS1	NM_006988	−2.5
ADAMTS4	NM_005099	46.6
ADAMTS5	NM_007038	−1.4
ADAMTS8	NM_007037	8.4
ADAMTS9	NM_182920	1.1
ADAMTS13	NM_139028	1.6
ADAMTS15	NM_139055	3.1
TIMP1	NM_003254	3.0
TIMP2	NM_003255	3.8
TIMP3	NM_000362	7.7

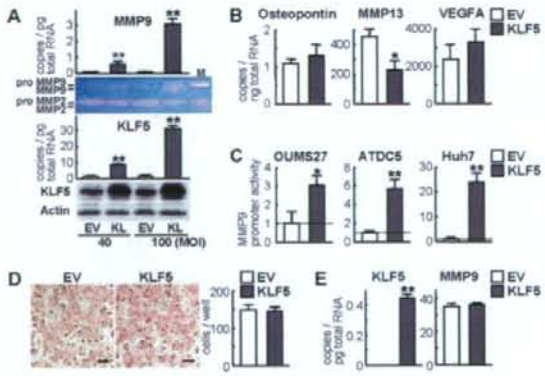

FIGURE 3. **Induction of MMP9 by KLF5 overexpression.** *A*, MMP9 and KLF5 mRNA levels determined by real time RT-PCR analysis after a 3-day culture of human chondrogenic OUMS27 cells adenovirally transfected with empty vector (*EV*) or KLF5 (*KL*) at 40 or 100 multiplicities of infection (*graphs*). Gelatinase activity was determined by gelatin zymography. The *right lane* (*M*) shows markers using recombinant proteins of pro-MMP9, pro-MMP2, and MMP2. KLF5 and actin protein levels were determined by Western blotting. *B*, osteopontin, MMP13, and VEGFA mRNA levels were determined by real time RT-PCR analysis in a 3-day culture of OUMS27 cells adenovirally transfected with 100 multiplicities of infection of EV or KLF5. *C*, MMP9 promoter activity determined by luciferase assay in OUMS27, ATDC5, and Huh7 cells co-transfected with a reporter construct containing the 1,250-bp MMP9 5′-end-flanking region and plasmid vector of EV or KLF5. Data are expressed as relative values compared with EV. *D*, TRAP staining of the osteoclast precursor M-BMMΦ that were retrovirally transfected with EV or KLF5 and cultured with M-CSF and RANKL for 4–5 days. *Scale bars*, 100 μm. The *graph* shows the number of TRAP-positive multinucleated osteoclasts. *E*, mRNA levels of KLF5 and MMP9 determined by real time RT-PCR analysis in the M-BMMΦ cultures. Data are expressed as means (*bars*) ± S.E. (*error bars*). *, $p < 0.05$; **, $p < 0.01$ *versus* EV.

MMP9 as a Transcriptional Target of KLF5 in Chondrocytes—To know the molecular mechanism whereby KLF5 contributes to cartilage degradation, we searched for the transcriptional targets by comparing mRNA levels in human chondrogenic cell line OUMS27 adenovirally transfected with KLF5 and the empty vector using microarray and real time RT-PCR analyses (Table 1). Among molecules related to matrix degradation, MMP9 expression was most strongly up-regulated by the KLF5 overexpression.

MMP9 mRNA level was confirmed to be increased in a dose-dependent manner of adenoviral KLF5 overexpression in OUMS27 cells (Fig. 3*A*). In addition, gelatin zymography revealed an increase of gelatin degradation by KLF5, which was compatible with MMP9 activity but not with MMP2 activity, indicating that KLF5 exhibited proteinase activity via the

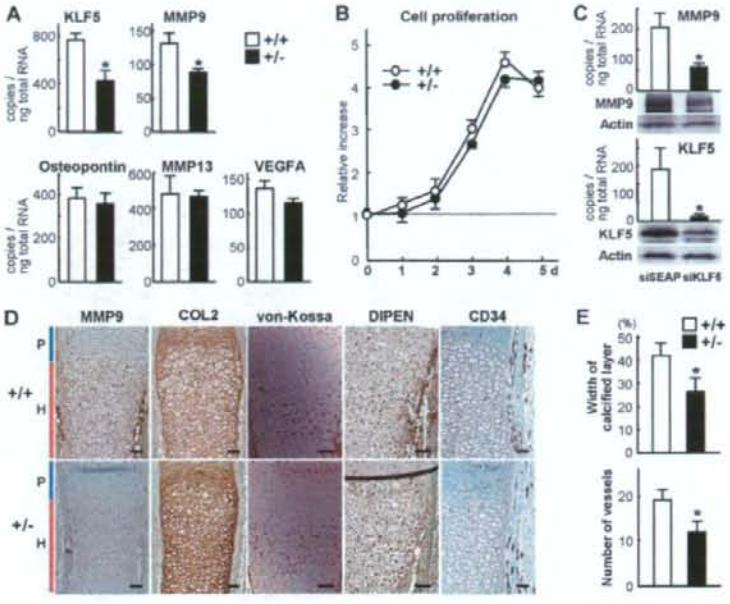

FIGURE 4. **Suppression of MMP9 by KLF5 insufficiency.** *A*, KLF5, MMP9, osteopontin, MMP13, and VEGFA mRNA levels determined by real time RT-PCR analysis in a 3-day culture of primary costal chondrocytes isolated from wild-type (+/+) and KLF5$^{+/-}$ littermates. Data are expressed as means (*bars*) ± S.E. (*error bars*) for 4 mice/group. *, $p < 0.05$ *versus* wild type. *B*, time course of the number of the primary costal chondrocytes above during 5 days of culture. Data are expressed as means (*symbols*) ± S.E. (*error bars*) of the ratios of day 0 for 3 wells/group. *C*, MMP9 and KLF5 mRNA levels determined by real time RT-PCR analysis after a 3-day culture of OUMS27 cells transfected with siSEAP (secreted form of the human placental alkaline phosphatase; control) or siKLF5 oligonucleotides (*graphs*). Data are expressed as means (*bars*) ± S.E. (*error bars*) for 3 wells/group. *, $p < 0.05$ *versus* siSEAP. MMP9, KLF5, and actin protein levels were determined by Western blotting. *D*, MMP9, COL2, DIPEN, and CD34 immunostainings and von Kossa staining of the tibial limbs of E15.5 wild-type and KLF5$^{+/-}$ embryos. *Blue* and *red bars* indicate proliferative (*P*) and hypertrophic (*H*) layers, respectively. *Scale bars*, 50 μm. *E*, the percentage width of the calcified layer to the entire hypertrophic layer determined by the von Kossa staining (*top*) and the number of blood vessels around the hypertrophic layer determined by the CD34 immunostaining (*bottom*) in the growth plates of E15.5 wild-type and KLF5$^{+/-}$ embryos. Data are expressed as means (*bars*) ± S.E. (error bars) for 3 mice/group. *, $p < 0.05$ *versus* wild type.

induction of MMP9. Contrarily, osteopontin mRNA level was not altered by the overexpression, suggesting that chondrocyte differentiation at later stages was not affected by KLF5 (Fig. 3*B*). MMP13 was moderately decreased, whereas vascular endothelial growth factor A (VEGFA) was little regulated by KLF5 in OUMS27 cells, both of which were consistent with the results of microarray analyses (Table 1 and supplemental Tables 1 and 2). To examine the transcriptional regulation, a luciferase reporter gene construct of the MMP9 5′-end-flanking region was transfected into OUMS27, ATDC5, and human hepatocytic Huh7 cells. The transcriptional activity determined by the luciferase reporter assay was enhanced by co-transfection with KLF5 in all cells, demonstrating the transcriptional induction of MMP9 by KLF5 (Fig. 3*C*).

The expression patterns of KLF5 and MMP-9 during chondrocyte differentiation were confirmed to be similar in cultured OUMS-27 cells (supplemental Fig. 1*A*). In addition, the time course analyses by immunostainings of embryonic limbs showed that KLF5 expression was seen early from E13.5, whereas MMP9 expression could be detected at E15.5 and enhanced at E16.5 (supplemental Fig. 1*B*). Since the embryonic stage when the suppression of cartilage degradation in the KLF5$^{+/-}$ limb was initiated around E16.5 (Fig. 2 and supplemental Fig. 2), these time courses support the hypothesis that MMP9 induction by KLF5 may lead to the cartilage degradation during endochondral ossification in skeletal development.

Since MMP9 is known to be strongly expressed in osteoclastic cells (26) and to play an important role in skeletal remodeling (3), we next investigated the effects of KLF5 on the culture of osteoclast precursor M-BMMΦ by retroviral overexpression of KLF5. Neither the osteoclastogenesis nor the MMP9 mRNA level was affected by the overexpression (Fig. 3, *D* and *E*). In the monocyte-macrophagic Raw264.7 cell culture as well, the adenoviral overexpression of KLF5 did not affect endogenous MMP9 mRNA level (supplemental Fig. 4*A*), whereas it increased the activity of the exogenously transfected luciferase reporter construct containing the MMP9 promoter above (supplemental Fig. 4*B*). These findings indicate that KLF5 does not have an important physiological function in osteoclastic cells.

To further examine the effect of loss of function of KLF5 in chondrocytes, we cultured primary costal chondrocytes derived from KLF5$^{+/-}$ mice and confirmed that the KLF5 mRNA level was decreased to about half that of wild-type chondrocytes (Fig. 4*A*). Among the molecules related to terminal differentiation of chondrocytes, cartilage degradation, and remodeling, only MMP9, and not osteopontin, MMP13, or VEGFA, was significantly suppressed by the KLF5 haploinsufficiency. Proliferative ability was comparable between cultured chondrocytes from KLF5$^{+/-}$ and the wild-type littermates (Fig. 4*B*). Gene silencing of KLF5 by RNA interference also caused the reduction of MMP9 mRNA expression in OUMS27 cells (Fig. 4*C*).

Finally, an immunohistochemical staining confirmed that MMP9 expression seen in the cartilage layer and the perichondrium of wild-type limb was scarcely detected in KLF5$^{+/-}$ (Fig. 4*D*). In the cartilage layer, the decreased MMP9 expression was correlated with the suppression of COL2 degradation and chondrocyte calcification, determined by immunohistochemical and von Kossa stainings, respectively. In the perichondrium, the MMP decrease was correlated with the suppression of DIPEN, which is a neoepitope at the aggrecan cleavage site generated by MMPs, and with that of CD34, which is an endothelial antigen representing blood vessels, determined by respective

immunostainings. Quantitative analyses actually revealed significant decreases in the width of the von Kossa-positive calcified layer and the number of CD34-positive blood vessels in the KLF5$^{+/-}$ limb (Fig. 4*E*).

DISCUSSION

The present *in vivo* analyses revealed that KLF5 haploinsufficiency caused impairment of cartilage matrix degradation and the subsequent remodeling to bone tissue, without affecting chondrocyte proliferation or differentiation. Microarray and cell culture analyses demonstrated that KLF5 contributes to the cartilage degradation through transcriptional induction of MMP9. MMP9 is known to be a potent proteinase that degrades denatured collagens and activates other MMPs and cytokines (4, 8, 27). In fact, the homozygous deficient mice (MMP9$^{-/-}$ mice) are reported to exhibit skeletal abnormality similar to KLF5$^{+/-}$ mice: elongation of hypertrophic layer, impaired vascularization, and delayed formation of bone and bone marrow cavity in the limbs (3), indicating a role of the KLF5-MMP9 axis during skeletal development.

It is, however, of note that the defect of KLF5 is physiologically more critical than that of MMP9, since KLF5$^{-/-}$ mice die *in utero* before E8.5, whereas MMP9$^{-/-}$ mice grow normally after birth, and MMP9$^{+/-}$ mice show no abnormality from embryos (3). This might be because KLF5 regulates molecules other than MMP9, since the present microarray analyses revealed up-regulation of several molecules like α-E-catenin (CTNNA1), ADAMTS4 (a disintegrin and metalloproteinase with thrombospondin-like repeat 4), interleukin-1, and MMP14 by the KLF5 overexpression in chondrogenic cells (Table 1 and supplemental Tables 1 and 2). α-E-catenin, a prototypic member of the α-catenin family and a component of the cadherin-catenin complex (28), is known to be required to sustain adhesion between cells during mammalian morphogenetic events (29). Although it is mainly expressed in epithelial tissues and the loss-of-function mutation causes human squamous cell carcinoma of the skin (30), the involvement in matrix degradation or angiogenesis remains unknown. Meanwhile, ADAMTS4 is a principal proteinase for aggrecan (31), a major cartilage matrix component that is degraded before collagenases cleave collagens in the hypertrophic layer (32). Hence, KLF5 might possibly lead to aggrecan degradation through induction of ADAMTS4, which is followed by matrix degradation by MMP9 (5). Interleukin-1, a representative proinflammatory cytokine, is also known to be a potent stimulator of MMPs, ADAMTSs, and other catabolic cytokines (32), so that interleukin-1 and MMP9 induced by KLF5 might initiate the subsequent catabolic changes of the cartilage. MMP14, although the induction by KLF5 was not strong (Table 1), is also a key proteinase in growth plate resorption, since the MMP-14-deficient mice exhibited dwarfism due to impaired endochondral ossification and angiogenesis, similarly to the KLF5$^{-/-}$ mice (33, 34). KLF5 may therefore be a crucial transcription factor that controls the molecular network for cartilage matrix degradation during endochondral ossification.

Another difference in the effects of insufficiency of KLF5 and MMP9 is their function in osteoclasts or chondroclasts. MMP9$^{-/-}$ mice showed abnormal bone remodeling after birth with impaired osteoclast recruitment, whereas KLF5$^{+/-}$ mice showed normal bone remodeling. Expression of MMP9 by osteoclastic cells may physiologically be important for skeletal development, since transplantation of wild-type bone marrow cells, including osteoclast progenitors, rescues the skeletal phenotype (3). In fact, MMP9 is abundantly expressed (26), whereas KLF5 was barely detected in osteoclastic cells (Fig. 1). The finding that the KLF5 overexpression in osteoclast precursors failed to alter endogenous MMP9 expression and osteoclastic differentiation (Fig. 3, *D* and *E*, and supplemental Fig. 4) supports the importance of MMP9 expression in osteoclastic cells. The present study, however, demonstrated that other than in osteoclasts, MMP9 was expressed in chondrocytes and perichondrium during skeletal development and was dramatically decreased by the KLF5 haploinsufficiency (Fig. 4*D*). This decrease was correlated with the suppression of COL2 degradation and an aggrecan cleavage neoepitope DIPEN. In addition, the induced MMP9 in chondrocytes by the KLF5 overexpression exerted a potent enzyme activity by gelatin zymography (Fig. 3*A*), as previously reported (35). These indicate a significant role of cell-autonomous action of MMP9 in chondrocytes in the process of cartilage degradation.

For endochondral ossification of hypertrophic chondrocytes, chondrocyte apoptosis, cartilage matrix degradation, and vascularization are tightly coupled (2, 5); however, which of these steps is rate-limiting remains unclear. A recent study on knockout mice of an antiapoptotic protein, galectin 3, has shown that acceleration of chondrocyte apoptosis was not associated with endochondral ossification (36), suggesting that chondrocyte apoptosis might be dispensable for the process. Several reports have indicated the matrix degradation and vascularization as the crucial steps (3, 5, 37–39), and, in fact, the present *in vivo* analyses showed that suppressions of MMP9 expression and cartilage matrix degradation by KLF5 insufficiency led to impairment of skeletal development accompanied by decreased vascularization (Fig. 4*D*). *In vitro* cultures, however, showed that a principal angiogenic factor, VEGFA (37–40), was little influenced by gain or loss of function of KLF5 in chondrocytes (Figs. 3*B* and 4*A*); nor were other angiogenic factors, VEGFC, VEGFD (41), HGF (42), FGF1, or FGF2 (43, 44), in the microarray analyses (supplemental Table 2). Hence, KLF5 is likely to regulate vascularization indirectly as a secondary effect of MMP9 secretion and matrix degradation in the cartilage layer and perichondrium, although the details need to be further investigated. In fact, cartilage explants from MMP9$^{-/-}$ mice in culture are reported to show a delayed angiogenesis (3). A previous report on MMP13$^{-/-}$ and MMP9$^{-/-}$ mice also showed that the cartilage matrix degradation was decreased in parallel with the pace that vasculature recruitment maintains with the slower rate of endochondral ossification (5). This evidence suggests that the matrix degradation may create a permissive environment for blood vessels to invade or make angiogenic factors accessible, leading to a hypothesis that cartilage degradation is a rate-limiting step for endochondral ossification of hypertrophic chondrocytes.

The skeletal abnormality of KLF5+/− mice was limited to the perinatal period and disappeared as the animals grew up after birth under physiological conditions. This may be due

to compensatory mechanisms for endochondral ossification, such as an increase of proteinases other than MMP9. In fact, proteinases, such as MMP13, tended to be regulated oppositely to MMP9 by the KLF5 overexpression (Fig. 3*B* and Table 1). Since MMPs are known to play roles under various pathological conditions, including wound healing, arthritis, and tumor development (45–47), we examined the effects of KLF5 insufficiency on bone fracture and arthritis by making the models in KLF5$^{+/-}$ mice at 8 weeks of age (supplemental Fig. 5, *A* and *B*). In results, there was no difference in fracture healing or arthritis development between KLF5$^{+/-}$ and the wild-type littermates. KLF5 may therefore be indispensable for skeletal development only in the perinatal period but be dispensable after birth under physiological and pathological conditions. Another possible compensatory mechanism is bone formation by osteoblasts, despite the expression of KLF5 in the cells (Fig. 1). This osteoblastic compensation may be sufficient to make up for the KLF5 dysfunction in chondrocytes after a substantial number of osteoblasts have appeared after birth but insufficient in the perinatal period when chondrocytes play central roles in endochondral ossification. Generation and evaluation of conditional knockout mice will clarify the tissue-specific roles of KLF5. In addition, further understanding of the molecular network related to the KLF5-MMP9 axis will greatly help us to unravel the complex mechanism modulating endochondral ossification.

REFERENCES

1. Kronenberg, H. M. (2003) *Nature* **423,** 332–336
2. Karsenty, G., and Wagner, E. F. (2002) *Dev. Cell* **2,** 389–406
3. Vu, T. H., Shipley, J. M., Bergers, G., Berger, J. E., Helms, J. A., Hanahan, D., Shapiro, S. D., Senior, R. M., and Werb, Z. (1998) *Cell* **93,** 411–422
4. Ortega, N., Behonick, D., Stickens, D., and Werb, Z. (2003) *Ann. N. Y. Acad. Sci.* **995,** 109–116
5. Stickens, D., Behonick, D. J., Ortega, N., Heyer, B., Hartenstein, B., Yu, Y., Fosang, A. J., Schorpp-Kistner, M., Angel, P., and Werb, Z. (2004) *Development* **131,** 5883–5895
6. Inada, M., Wang, Y., Byrne, M. H., Rahman, M. U., Miyaura, C., Lopez-Otin, C., and Krane, S. M. (2004) *Proc. Natl. Acad. Sci. U. S. A.* **101,** 17192–17197
7. Lee, E. R., Murphy, G., El-Alfy, M., Davoli, M. A., Lamplugh, L., Docherty, A. J., and Leblond, C. P. (1999) *Dev. Dyn.* **215,** 190–205
8. Werb, Z. (1997) *Cell* **91,** 439–442
9. Kaczynski, J., Cook, T., and Urrutia, R. (2003) *Genome Biol.* **4,** 206
10. van Vliet, J., Crofts, L. A., Quinlan, K. G., Czolij, R., Perkins, A. C., and Crossley, M. (2006) *Genomics* **87,** 474–482
11. Bieker, J. J. (2001) *J. Biol. Chem.* **276,** 34355–34358
12. Watanabe, N., Kurabayashi, M., Shimomura, Y., Kawai-Kowase, K., Hoshino, Y., Manabe, I., Watanabe, M., Aikawa, M., Kuro-o, M., Suzuki, T., Yazaki, Y., and Nagai, R. (1999) *Circ. Res.* **85,** 182–191
13. Ohnishi, S., Laub, F., Matsumoto, N., Asaka, M., Ramirez, F., Yoshida, T., and Terada, M. (2000) *Dev. Dyn.* **217,** 421–429
14. Conkright, M. D., Wani, M. A., Anderson, K. P., and Lingrel, J. B (1999) *Nucleic Acids Res.* **27,** 1263–1270
15. Shindo, T., Manabe, I., Fukushima, Y., Tobe, K., Aizawa, K., Miyamoto, S., Kawai-Kowase, K., Moriyama, N., Imai, Y., Kawakami, H., Nishimatsu, H., Ishikawa, T., Suzuki, T., Morita, H., Maemura, K., Sata, M., Hirata, Y., Komukai, M., Kagechika, H., Kadowaki, T., Kurabayashi, M., and Nagai, R. (2002) *Nat. Med.* **8,** 856–863
16. Oishi, Y., Manabe, I., Tobe, K., Tsushima, K., Shindo, T., Fujiu, K., Nishimura, G., Maemura, K., Yamauchi, T., Kubota, N., Suzuki, R., Kitamura, T., Akira, S., Kadowaki, T., and Nagai, R. (2005) *Cell Metab.* **1,** 27–39
17. Gollner, H., Dani, C., Phillips, B., Philipsen, S., and Suske, G. (2001) *Mech. Dev.* **106,** 77–83
18. Nakashima, K., Zhou, X., Kunkel, G., Zhang, Z., Deng, J. M., Behringer, R. R., and de Crombrugghe, B. (2002) *Cell* **108,** 17–29
19. Lefebvre, V., Garofalo, S., Zhou, G., Metsaranta, M., Vuorio, E., and De Crombrugghe, B. (1994) *Matrix Biol.* **14,** 329–335
20. Kobayashi, K., Takahashi, N., Jimi, E., Udagawa, N., Takami, M., Kotake, S., Nakagawa, N., Kinosaki, M., Yamaguchi, K., Shima, N., Yasuda, H., Morinaga, T., Higashio, K., Martin, T. J., and Suda, T. (2000) *J. Exp. Med.* **191,** 275–286
21. Aizawa, K., Suzuki, T., Kada, N., Ishihara, A., Kawai-Kowase, K., Matsumura, T., Sasaki, K., Munemasa, Y., Manabe, I., Kurabayashi, M., Collins, T., and Nagai, R. (2004) *J. Biol. Chem.* **279,** 70–76
22. Shimoaka, T., Kamekura, S., Chikuda, H., Hoshi, K., Chung, U. I., Akune, T., Maruyama, Z., Komori, T., Matsumoto, M., Ogawa, W., Terauchi, Y., Kadowaki, T., Nakamura, K., and Kawaguchi, H. (2004) *J. Biol. Chem.* **279,** 15314–15322
23. Yamada, T., Kawano, H., Koshizuka, Y., Fukuda, T., Yoshimura, K., Kamekura, S., Saito, T., Ikeda, T., Kawasaki, Y., Azuma, Y., Ikegawa, S., Hoshi, K., Chung, U. I., Nakamura, K., Kato, S., and Kawaguchi, H. (2006) *Nat. Med.* **12,** 665–670
24. Terato, K., Harper, D. S., Griffiths, M. M., Hasty, D. L., Ye, X. J., Cremer, M. A., and Seyer, J. M. (1995) *Autoimmunity* **22,** 137–147
25. Terato, K., Hasty, K. A., Reife, R. A., Cremer, M. A., Kang, A. H., and Stuart, J. M. (1992) *J. Immunol.* **148,** 2103–2108
26. Reponen, P., Sahlberg, C., Munaut, C., Thesleff, I., and Tryggvason, K. (1994) *Ann. N. Y. Acad. Sci.* **732,** 472–475
27. Engsig, M. T., Chen, Q. J., Vu, T. H., Pedersen, A. C., Therkidsen, B., Lund, L. R., Henriksen, K., Lenhard, T., Foged, N. T., Werb, Z., and Delaisse, J. M. (2000) *J. Cell Biol.* **151,** 879–889
28. Perez-Moreno, M., and Fuchs, E. (2006) *Dev. Cell* **11,** 601–612
29. Torres, M., Stoykova, A., Huber, O., Chowdhury, K., Bonaldo, P., Mansouri, A., Butz, S., Kemler, R., and Gruss, P. (1997) *Proc. Natl. Acad. Sci. U. S. A.* **94,** 901–906
30. Kobielak, A., and Fuchs, E. (2006) *Proc. Natl. Acad. Sci. U. S. A.* **103,** 2322–2327
31. Tortorella, M. D., Burn, T. C., Pratta, M. A., Abbaszade, I., Hollis, J. M., Liu, R., Rosenfeld, S. A., Copeland, R. A., Decicco, C. P., Wynn, R., Rockwell, A., Yang, F., Duke, J. L., Solomon, K., George, H., Bruckner, R., Nagase, H., Itoh, Y., Ellis, D. M., Ross, H., Wiswall, B. H., Murphy, K., Hillman, M. C., Jr., Hollis, G. F., Newton, R. C., Magolda, R. L., Trzaskos, J. M., and Arner, E. C. (1999) *Science* **284,** 1664–1666
32. Pratta, M. A., Yao, W., Decicco, C., Tortorella, M. D., Liu, R. Q., Copeland, R. A., Magolda, R., Newton, R. C., Trzaskos, J. M., and Arner, E. C. (2003) *J. Biol. Chem.* **278,** 45539–45545
33. Holmbeck, K., Bianco, P., Caterina, J., Yamada, S., Kromer, M., Kuznetsov, S. A., Mankani, M., Robey, P. G., Poole, A. R., Pidoux, I., Ward, J. M., and Birkedal-Hansen, H. (1999) *Cell* **99,** 81–92
34. Zhou, Z., Apte, S. S., Soininen, R., Cao, R., Baaklini, G. Y., Rauser, R. W., Wang, J., Cao, Y., and Tryggvason, K. (2000) *Proc. Natl. Acad. Sci. U. S. A.* **97,** 4052–4057
35. Haeusler, G., Walter, I., Helmreich, M., and Egerbacher, M. (2005) *Calcif. Tissue Int.* **76,** 326–335
36. Colnot, C., Sidhu, S. S., Balmain, N., and Poirier, F. (2001) *Dev. Biol.* **229,** 203–214
37. Gerber, H. P., Vu, T. H., Ryan, A. M., Kowalski, J., Werb, Z., and Ferrara, N. (1999) *Nat. Med.* **5,** 623–628
38. Maes, C., Carmeliet, P., Moermans, K., Stockmans, I., Smets, N., Collen, D., Bouillon, R., and Carmeliet, G. (2002) *Mech. Dev.* **111,** 61–73
39. Zelzer, E., Mamluk, R., Ferrara, N., Johnson, R. S., Schipani, E., and Olsen, B. R. (2004) *Development* **131,** 2161–2171
40. Zelzer, E., McLean, W., Ng, Y. S., Fukai, N., Reginato, A. M., Lovejoy, S., D'Amore, P. A., and Olsen, B. R. (2002) *Development* **129,** 1893–1904
41. Bluteau, G., Julien, M., Magne, D., Mallein-Gerin, F., Weiss, P., Daculsi, G., and Guicheux, J. (2007) *Bone* **40,** 568–576
42. Naldini, L., Vigna, E., Bardelli, A., Follenzi, A., Galimi, F., and Comoglio, P. M. (1995) *J. Biol. Chem.* **270,** 603–611

43. Jingushi, S., Scully, S. P., Joyce, M. E., Sugioka, Y., and Bolander, M. E. (1995) *J. Orthop. Res.* **13,** 761–768
44. Whitelock, J. M., Murdoch, A. D., Iozzo, R. V., and Underwood, P. A. (1996) *J. Biol. Chem.* **271,** 10079–10086
45. Milner, J. M., and Cawston, T. E. (2005) *Curr. Drug Targets Inflamm. Allergy* **4,** 363–375
46. Colnot, C., Thompson, Z., Miclau, T., Werb, Z., and Helms, J. A. (2003) *Development* **130,** 4123–4133
47. Kosaki, N., Takaishi, H., Kamekura, S., Kimura, T., Okada, Y., Minqi, L., Amizuka, N., Chung, U. I., Nakamura, K., Kawaguchi, H., Toyama, Y., and D'Armiento, J. (2007) *Biochem. Biophys. Res. Commun.* **354,** 846–851

Osteoarthritis and Cartilage (2008) **16**, 1300–1306

doi:10.1016/j.joca.2008.03.011

Osteoarthritis and Cartilage

International Cartilage Repair Society

OARSI OSTEOARTHRITIS

Fully automatic quantification of knee osteoarthritis severity on plain radiographs

H. Oka M.D.†, S. Muraki M.D., Ph.D.†, T. Akune M.D., Ph.D.†, A. Mabuchi M.D., Ph.D.†, T. Suzuki M.D., Ph.D.‡, H. Yoshida M.D., Ph.D.‡, S. Yamamoto M.D., Ph.D.‡, K. Nakamura M.D., Ph.D.§, N. Yoshimura M.D., Ph.D.† and H. Kawaguchi M.D., Ph.D.§*

† *22nd Century Medical Center, The University of Tokyo, Tokyo, Japan*

‡ *Tokyo Metropolitan Institute of Gerontology, Tokyo, Japan*

§ *Sensory and Motor System Medicine, The University of Tokyo, Tokyo, Japan*

Summary

Objective: Although knee osteoarthritis (OA) is a major public health issue causing chronic disability, there is no objective or accurate method for measurement of the structural severity in general clinical practice. Here we have established a fully automatic program KOACAD (knee OA computer-aided diagnosis) to quantify the major OA parameters on plain knee radiographs, validated the reproducibility and reliability, and investigated the association of the parameters with knee pain.

Methods: KOACAD was programmed to measure joint space narrowing at medial and lateral sides, osteophyte formation, and joint angulation. Anteroposterior radiographs of 1979 knees of a large-scale cohort population were analyzed by KOACAD and conventional categorical grading systems.

Results: KOACAD automatically measured all parameters in less than 1 s without intra- or interobserver variability. All parameters, especially medial joint space narrowing, were significantly correlated with the conventional gradings. In the parameters, osteophyte formation was associated with none of the joint space parameters, suggesting different etiologic mechanisms between them. Multivariate logistic regression analysis after adjustment for age and confounding factors revealed that medial joint space narrowing and varus angulation of knee joints were risk factors for the presence of pain (594/1979 knees), while neither lateral joint space nor osteophyte area was.

Conclusion: KOACAD was shown to be useful for objective, accurate, simple and easy evaluation of the radiographic knee OA severity in daily clinical practice. This system may also serve as a surrogate measure for the development of disease-modifying drugs for OA, just as bone mineral density does in osteoporosis.

Key words: Osteoarthritis, Knee, Diagnosis, Computer-aided diagnosis, Imaging, Plain radiograph.

Introduction

Due to the rapidly increasing fraction of aging people today, osteoarthritis (OA) is now considered as a major public health issue causing chronic disability in most developed countries. It is estimated that up to 10% of the entire world population, and more than 50% of those aged over 50 years, are suffering from OA[1]. Knee OA, affecting about 30% of those over 65 years and as often associated with disability as heart and chronic lung diseases[2,3], is characterized by pathological features including joint space narrowing, osteophyte formation, and joint angulation. Although OA and osteoporosis are the two major skeletal disorders with strong social impact[4], OA falls far behind osteoporosis in the assessment of its disease severity and in the development of disease-modifying drugs. This is mainly due to the lack of an objective and accurate method to evaluate the structural severity and thereby to assess the efficacy of drugs as surrogate measures like bone mineral density (BMD) in osteoporosis.

Although magnetic resonance imaging (MRI) with high resolution has been rapidly advanced as a promising technique, it is still too laborious and expensive to perform in general clinical practice or in population-based epidemiologic studies, and the interpretation remains controversial as a primary end-point in clinical trials of the disease-modifying drugs[5–7]. Biochemical markers of cartilage turnover are being tested to measure the disease progression; however, their validation as a surrogate measure will require significant additional work[5,8]. Hence, plain radiography is considered the gold standard as a method that is non-invasive, inexpensive, convenient, simple, and fast to use in assessing OA severity. The most conventional system to grade the radiographic severity has been the Kellgren/Lawrence (K/L) grading[9]. However, this categorical system is limited by incorrect assumptions that progression of distinct OA features like joint space narrowing and osteophyte formation is linear and constant, and that their relationships are proportional. Since the system emphasizes the development of osteophytes, it is unclear how to handle knees with severe joint space narrowing but no osteophyte formation. To overcome the problem,

*Address correspondence and reprint requests to: Dr Hiroshi Kawaguchi, M.D., Ph.D., Sensory and Motor System Medicine, Faculty of Medicine, The University of Tokyo, Hongo 7-3-1, Bunkyo, Tokyo 113-8655, Japan. Tel: 81-3-3815-5411 ext. 30473; Fax: 81-3-3818-4082; E-mail: kawaguchi-ort@h.u-tokyo.ac.jp

Received 3 January 2008; revision accepted 9 March 2008.

a radiographic atlas of individual features was published by the OA Research Society International (OARSI) in 1995[10] and a revised version in 2007[11]. This system separately evaluates joint space narrowing and osteophyte formation at the medial and lateral tibiofemoral compartments on radiographs; however, the grading is still limited in reproducibility and sensitivity due to the subjective judgment of individual observers and the categorical classification into four-grade (0–3) scales. Although several semi-automatic methods for objective measurement with continuous variables of joint space or angle using computer-assisted systems have recently been developed, there still remain intra- and interobserver variabilities since initial operations like identifying points or drawing lines must be manually performed[12–16].

The present study has developed a novel computer program, KOACAD (knee OA computer-aided diagnosis), which for the first time has realized a fully automatic measurement of major parameters of knee OA: joint space area (JSA) and the minimum joint space width (mJSW) at medial and lateral sides, osteophyte area, and tibiofemoral angle (TFA) on plain anteroposterior radiographs. We examined the reproducibility and reliability of KOACAD by comparing it with conventional grading systems and semi-automatic measurements.

Arthritis is the most common cause of pain in the elderly[17], and knee pain is the principal clinical symptom of knee OA. Although much effort has been devoted toward a definition of knee pain, the correlation with radiographic severity of the knee OA was not as strong as one would expect[18–20]. Hence, this study finally sought to identify radiographic factors related to knee pain by examining the association of the KOACAD parameters with the presence of pain using a baseline database of our large-scale OA cohort study ROAD (research on OA against disability).

Subjects and methods

SUBJECTS

The ROAD study is a nationwide OA cohort study that started in 2005, and is constituted of four cohorts. So far, we have completed creation of a baseline database including clinical and genomic information of 3040 participants in three cohorts in urban, mountainous, and seacoast areas. The database includes anteroposterior and lateral radiographs of bilateral knees of all participants. For evaluation of the KOACAD system, we used 1979 anteroposterior radiographs from 2002 knees of 1001 participants of the urban cohort after 15 artificial knee joints and eight knees with more than 5° flexion contracture were omitted. The study was conducted with approval of the Institutional Review Boards (IRBs) of the University of Tokyo and the Tokyo Metropolitan Institute of Gerontology, and all participants provided written informed consent.

RADIOGRAPHY

Plain radiographs with standing on both legs and the knee extended were taken with a horizontal X-ray beam unless otherwise described, using a Fuji 5000 Plus Reader on a 36 × 46 cm Fuji ST-VI Computed Radiography (CR) imaging plate (Fuji Medical Systems, Tokyo, Japan) with a 20 × 30 mm rectangular metal plate beside it as a magnification index. Rotation of the foot was adjusted to keep the second metatarsal bone parallel to the X-ray beam. Images were downloaded into Digital Imaging and Communication in Medicine (DICOM) format files with a spatial resolution of 1584 × 2016 pixels (giving a pixel size of 0.01 mm) and 1024 gray levels.

IMAGE PROCESSING BY KOACAD

The KOACAD was programmed to perform the following operations automatically on the digital images above using the object-oriented programming language C++ [Fig. 1(A)]. Initially, correction for radiographic magnification was performed based on the image size of the rectangular metal plate. To reduce the image noise, the entire radiograph underwent filtering three times with a 3 × 3 square neighborhood median filter as reported previously[21]. Then, the Robert's filter was applied to extract the rough outlines of tibia and femur, so that medial and lateral sides could be judged by the difference of calculated widths of tibia and fibula at the level of 100 pixels above the bottom of the image [Fig. 1(B)].

Next, to determine the region of interest (ROI) including the tibiofemoral joint space, a vertical neighborhood difference filter was applied to identify points with high absolute values of difference of scales. The center of all the points was then calculated, and 480 × 200 pixels of a rectangle with the center was decided as the ROI [Fig. 1(C)]. Within the ROI, the outline of femoral condyle was designated as the upper rim of the joint space by vertical filtering with the 3 × 3 square neighborhood difference filter [Fig. 1(D)]. The two ends were determined using a Canny's filter to remove the noise of lines[22], and vertical lines from the ends were designated as the outside rims of the joint space. Outlines of anterior and posterior margins of the tibial plateau were drawn similarly to that of the femoral condyle, and the middle line between the two outlines was designated as the lower rim of the joint space [Fig. 1(E)]. Then, a straight regression line for the lower rim outline was drawn, and their intersections were designated as the inside rims [Fig. 1(F)]. The medial and lateral JSAs were determined as the areas surrounded by the upper, lower, inside, and outside rims above [Fig. 1(G)]. The medial and lateral mJSWs were further determined as the minimum vertical distances in the respective JSA [Fig. 1(H)].

To measure osteophyte area and TFA, the medial and lateral outlines of femur and tibia were drawn by the 3 × 3 square horizontal neighborhood difference filter and Canny's filter as described above. Then, the inflection points for the outlines were calculated. The medial outline of the tibia from the inflection point was drawn upward to the joint level [Fig. 1(I)], and the area that was medially prominent over the smoothly extended outline was designated as the osteophyte area [Fig. 1(J)]. For TFA, a middle line between the medial and lateral outlines of the femur from the top of the image to the inflection points was drawn [Fig. 1(K)], and the straight regression line was determined to be the axis of the femur. Similarly, the straight regression line of the middle line of the tibia from the bottom to the inflection points was designated as the axis of the tibia. The lateral angle between the two axis lines was calculated as TFA [Fig. 1(L)].

ANALYSES

To decide the ideal conditions for the taking of radiographs for the KOACAD analysis, we initially evaluated the reproducibility of the six parameters by an intraclass coefficient of correlation (ICC) on radiographs of 20 individuals taken at a 2-week interval with various knee flexion angles (0, 10, 20, and 30°) and X-ray beam angulations (0, 5, 10, and 15°).

Conventional gradings by the K/L system and the OARSI radiographic atlas were performed by experienced orthopedists on 50 radiographs randomly selected from the 1979 radiographs above, and intra- and interobserver variabilities were evaluated by κ values. The KOACAD parameters were also evaluated by semi-automatic measurement by a conventional computer-assisted program (Quick Grain Standard, Inotech, Hiroshima, Japan) after drawing of the outlines of femur and tibia by the orthopedists, and intra- and interobserver ICCs of each parameter were compared with those of KOACAD.

Correlations of the KOACAD parameters with the K/L grading (0–4) were examined by Spearman's correlation test on the entire 1979 radiographs. Correlations with the OARSI grading (0–3) were similarly examined for five common parameters: the KOACAD mJSW and JSA at the medial and lateral sides were compared with the OARSI joint space narrowing grades at the respective sides, and the KOACAD osteophyte area with the OARSI osteophyte grade of the medial tibial plateau. Since there was no radiograph of OARSI grade 3 of lateral joint space narrowing, correlations of the KOACAD lateral JSA and lateral mJSW were examined with the OARSI grade 0–2.

Correlations among the KOACAD parameters were analyzed using Pearson's correlation test, and parameters with correlation value of more than 0.5 were defined as confounding factors.

For the assessment of factors associated with symptomatic knee pain, age and the six KOACAD parameters were compared between knees with and without pain by Student's *t* test on the 1979 radiographs. Logistic regression analyses were used to estimate odds ratio (OR) and the associated 95% confidence interval (CI). Final multivariate logistic models were created through stepwise elimination of variables of interest from univariate analysis after adjustment for age and confounding factors.

A *P*-value of <0.05 for analysis of safety variables was considered significant. Data analyses were performed using SAS version 9.0 (SAS Institute Inc., NC, USA).

Results

REPRODUCIBILITY OF KOACAD PARAMETERS BY KNEE FLEXION ANGLES AND X-RAY BEAM ANGULATIONS

The KOACAD system could automatically measure the six parameters on an anteroposterior knee radiograph in

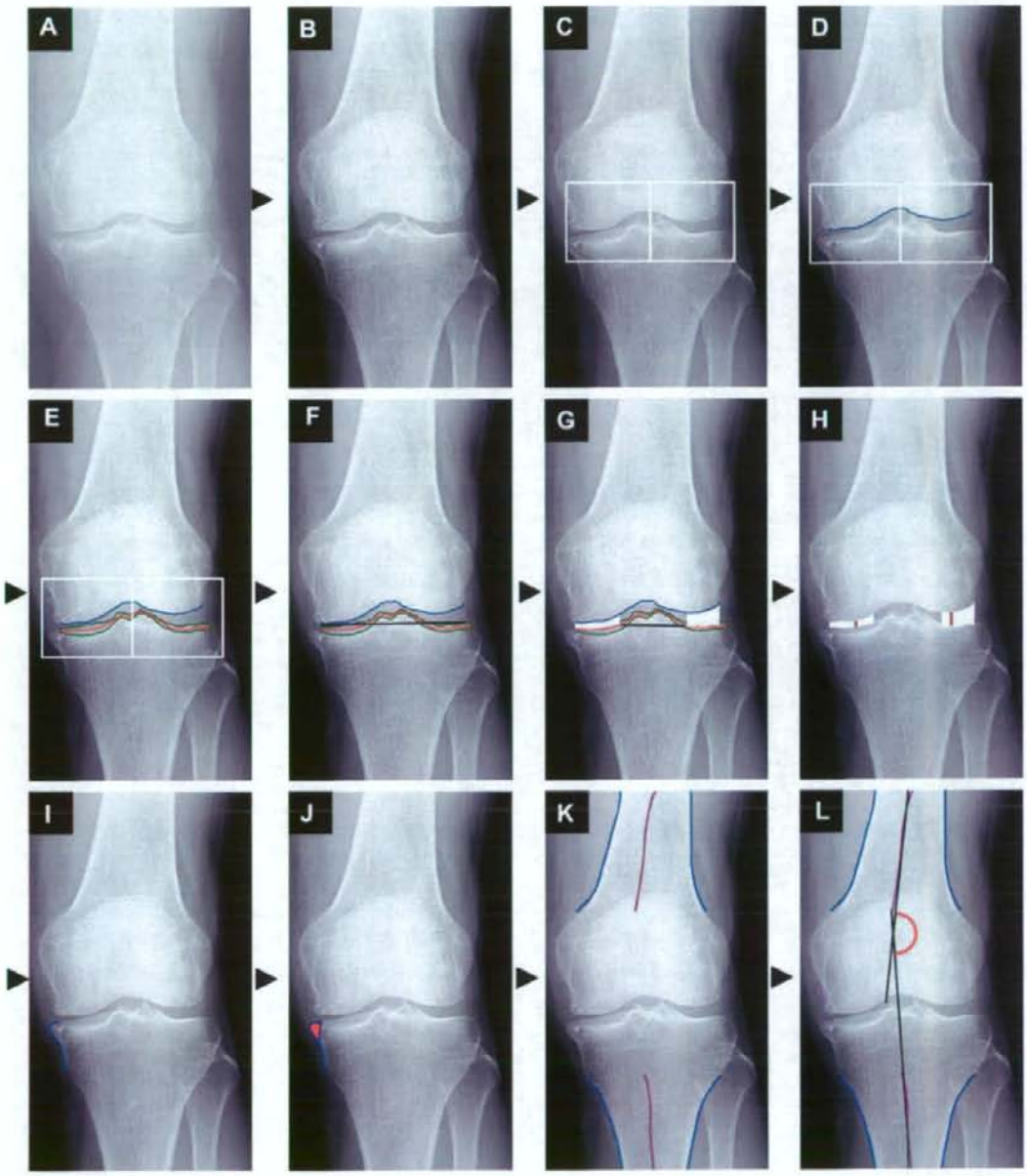

Fig. 1. Schema of image processing by KOACAD. (A) A digitized knee radiograph as a DICOM file. (B) Filterings to reduce the image noise and to extract outlines of tibia and femur. (C) ROI and the center including the tibiofemoral joint space. (D) An outline of femoral condyle (blue line) as the upper and outside rims of the joint space. (E) Outlines of anterior and posterior margins of the tibial plateau (green lines), and the middle line between the two outlines (red line) as the lower rim of the joint space. (F) A straight regression line (black line) for the lower rim line, and their intersections as the inside rims. (G) Medial and lateral JSAs (white areas) surrounded by the upper, lower, inside, and outside rims. (H) Medial and lateral mJSWs (brown lines) as the minimum vertical distances in the JSAs. (I) Medial outline (blue line) of the tibia drawn from the calculated inflection point upward to the joint level. (J) Osteophyte area (red area) that is medially prominent over the smoothly extended outline of the tibia. (K) Medial and lateral outlines (blue lines) of the femur and tibia from the edges of the image to the inflection points, and the middle lines (purple lines). (L) TFA as the lateral angle between the straight regression lines (black lines) of the middle lines above in the femur and tibia.

less than 1 s without any manual operation. To decide the ideal conditions of taking radiographs for the KOACAD analysis, we first examined the reproducibility of the parameters measured on radiographs of 20 individuals taken at a 2-week interval with various knee flexion angles and X-ray beam angulations (Table I). The reproducibility of all parameters was highly maintained with 0° of the knee flexion angle (ICC = 0.88–0.99), which became lower as the angle was increased. It was also maintained with 0 and 5° of X-ray beam angulations (ICC = 0.87–0.99), while it was not determined in most of the radiographs with 10 and 15° due to overlap of femoral condyle and tibial plateau. Hence, we decided to take radiographs with the knee extended and a horizontal X-ray beam for the KOACAD measurement.

COMPARISON OF KOACAD WITH CONVENTIONAL SYSTEMS

We measured the six parameters by KOACAD more than twice on 1979 radiographs, and confirmed that all parameters were unchanged independent of observer or time measured (all ICC = 1.0). Contrarily, when we examined the intra- and interobserver variabilities of the conventional categorical grading systems on 50 randomly selected radiographs, the intra- and interobserver variabilities were high by the K/L system (κ value = 0.84 and 0.76) and the OARSI radiographic atlas ($\kappa \leq 0.75$ and ≤ 0.65) (Supplementary Table S1). In addition, the intra- and interobserver ICCs of semi-automatic measurements using a conventional computer-assisted procedure of the parameters were less than 0.7 and 0.6, respectively, for joint space parameters and osteophyte area, and were less than 0.8 for TFA, indicating that even this computer-assisted system is robust with respect to variability in lines drawn by observers for the computer to analyze (Supplementary Table S1).

We then examined the correlations of the KOACAD parameters with the K/L and OARSI gradings on the 1979 radiographs (Table II). All parameters were significantly correlated with the K/L grading ($P < 0.0001$); with medial JSA, medial mJSW, and TFA being most strongly correlated with it. Five common parameters showed good correlation between KOACAD and OARSI grading ($P < 0.0001$), and medial JSA and medial mJSW also showed most of the strong correlations.

CORRELATIONS AMONG THE KOACAD PARAMETERS

Although all KOACAD parameters are known to be affected as OA progresses, the changes are neither proportional nor is the relationship constant. We therefore examined the correlations among the parameters on the 1979 radiographs by Pearson's correlation test (Table III). As expected, correlation values were more than 0.5 between medial JSA and medial mJSW, and between lateral JSA and lateral mJSW, indicating that these are confounding factors for each other. More interestingly, although osteophyte area was measured at the medial tibia, it was significantly associated with neither medial JSA nor mJSW, suggesting different etiologic mechanisms between osteophyte formation and joint destruction. Furthermore, JSA and mJSW at the lateral side were positively correlated with those at the medial side, and TFA was strongly associated with decreased mJSWs not only at the medial side but also at the lateral side. This implies that there is a background generally affecting the whole joint for OA progression rather than the medial-lateral shift of loading axis of mechanical stress within the joint.

CORRELATIONS OF THE KOACAD PARAMETERS WITH KNEE PAIN

To further identify radiographic factors associated with knee pain using the KOACAD system in the 1979 radiographs, we compared the parameters between groups with (594 knees) and without (1385 knees) knee pain (Table IV). Although age was comparable, all parameters were significantly different between the two groups. Especially, medial JSA and medial mJSW were lower and TFA was higher in the group with pain than that without pain. Univariate logistic regression analysis after adjustment for age revealed that female sex (OR = 1.64; 95% CI = 1.47–1.84), medial JSA (1.16; 1.05–1.27), medial mJSW (1.66; 1.49–1.87), and TFA (1.07; 1.03–1.10) were significantly associated with the presence of pain.

Considering that medial mJSW and medial JSA, as well as lateral mJSW and lateral JSA, were found to be confounders for each other (Pearson's correlation value > 0.5; Table III), we performed a multivariate analysis after adjustment for age and confounding factors in both genders

Table I

Reproducibility of KOACAD parameters measured on radiographs of an individual with various knee flexion angles and X-ray beam angulations

Knee flexion angle (°)	0	10	20	30
KOACAD parameters (ICC)				
Medial JSA (mm^2)	0.88	0.77	0.74	0.74
Lateral JSA (mm^2)	0.92	0.87	0.73	0.73
Medial mJSW (mm)	0.96	0.92	0.90	0.78
Lateral mJSW (mm)	0.95	0.86	0.88	0.80
Osteophyte area (mm^2)	0.99	0.91	0.79	0.81
TFA (°)	0.94	0.93	0.86	0.86
X-ray beam angulation (°)	0	5	10	15
KOACAD parameters (ICC)				
Medial JSA (mm^2)	0.88	0.87	ND	ND
Lateral JSA (mm^2)	0.92	0.92	(17/20)	(20/20)
Medial mJSW (mm)	0.96	0.96		
Lateral mJSW (mm)	0.95	0.95		
Osteophyte area (mm^2)	0.99	0.99		
TFA (°)	0.94	0.93		

Reproducibility of six parameters was evaluated by an ICC on radiographs of 20 individuals taken at a 2-week interval. ND: not determined due to overlap of femur and tibia.

Table II
Correlations of the KOACAD parameters with the K/L and OARSI gradings

	0	1	2	3	4	R^2
K/L grading						
Number	162	625	956	205	31	
Medial JSA (mm^2)	112.4 ± 1.8	97.0 ± 0.9	91.1 ± 0.7	83.2 ± 1.9	52.4 ± 5.4	−0.29
Lateral JSA (mm^2)	114.3 ± 2.0	110.6 ± 1.1	107.2 ± 0.9	105.3 ± 1.9	106.2 ± 6.1	−0.09
Medial mJSW (mm)	3.9 ± 0.1	3.4 ± 0.0	3.1 ± 0.0	2.5 ± 0.1	1.5 ± 0.2	−0.41
Lateral mJSW (mm)	4.7 ± 0.1	4.4 ± 0.0	4.3 ± 0.1	4.2 ± 0.1	4.2 ± 0.3	−0.11
Osteophyte area (mm^2)	2.7 ± 1.4	2.0 ± 0.2	3.2 ± 0.2	7.9 ± 1.3	10.9 ± 4.2	0.15
TFA (°)	175.7 ± 0.2	176.2 ± 0.1	177.4 ± 0.1	179.6 ± 0.3	184.2 ± 1.2	0.31
OARSI grading						
Medial JSA (mm^2) (n)	105.9 ± 0.9 (602)	89.8 ± 0.7 (953)	90.0 ± 1.3 (317)	65.4 ± 2.2 (107)		−0.34
Lateral JSA (mm^2) (n)	109.6 ± 0.6 (1926)	87.7 ± 4.2 (38)	61.7 ± 7.3 (15)	− (0)		−0.16
Medial mJSW (mm) (n)	3.6 ± 0.0 (602)	3.1 ± 0.0 (953)	2.7 ± 0.0 (317)	1.8 ± 0.1 (107)		−0.45
Lateral mJSW (mm) (n)	4.3 ± 0.0 (1926)	3.3 ± 0.2 (38)	2.5 ± 0.3 (15)	− (0)		−0.19
Osteophyte area (mm^2) (n)	2.0 ± 0.2 (1212)	2.8 ± 0.4 (421)	4.7 ± 0.6 (215)	14.7 ± 0.7 (131)		0.25

Analyses were performed by Spearman's correlation test on 1979 radiographs, and data are expressed by means ± S.E.M. (all *P*-values < 0.0001).

(Table V). It was found that low medial mJSW and high TFA were associated with the presence of pain, while neither lateral mJSW nor osteophyte area was.

Discussion

In the present study, we established a fully automatic computer-assisted program, KOACAD that can quantitate the major features of knee OA on plain radiographs. This system has achieved objective, accurate, simple and easy assessment of the structural severity of knee OA without any manual operation in general clinical practice or in population-based epidemiologic studies. The system could also accurately evaluate distinct features of knee OA like joint space narrowing, osteophyte formation, and joint angulation in one sitting. By applying this system to the baseline data in the ROAD study, medial joint space narrowing and varus angulation, though neither lateral joint space narrowing nor osteophyte formation, was shown to be associated with symptomatic knee pain.

Independent measurement of the parameters by KOACAD enabled us to examine the correlation of distinct features of OA, which may lead to better understanding of the OA pathophysiology. For example, a lack of association between osteophyte formation and joint space narrowing indicates independent backgrounds of the two representative features of knee OA. A previous prospective study using a famous OA cohort, the Chingford study, has reported that there was no association between the two features[23]. Although the authors described in the paper that this might possibly be due to inaccurate and subjective measurement on radiographs, the present KOACAD analysis has confirmed the reliability by accurate and objective measurement. A recent cross-sectional study has also shown that osteophyte formation was unrelated not only to joint space narrowing on plain radiographs, but also to cartilage loss measured by quantitative MRI[24]. Furthermore, by creating an OA model through induction of instability in mouse knee joints, we have identified a cartilage specific molecule, carminerin, that regulates osteophyte formation without affecting cartilage destruction during the OA progression[25,26]. Further clinical and basic research will disclose the distinct backgrounds of the two OA features. The correlation analysis among the parameters also revealed that joint space narrowing at medial and lateral sides was positively correlated, indicating an etiologic mechanism that affects the whole joint. Although this does not necessarily deny the mechanistic contribution of medial-lateral shift of the loading axis within the joint to the OA progression, the limitation of efficacy of a valgus knee brace, lateral wedged insole, or valgus high tibial osteotomy for medial compartment OA of the knee may at least partly be explained by the result.

For accurate and reproducible assessment of tibiofemoral joint space on plain radiographs, a variety of radiographic methods have been developed. Several reports have claimed that positioning of the knee with several angles of flexion provides more accurate joint space measurement than conventional extended knees due to superimposition of the anterior and posterior margins of the tibial plateau[13,27,28]. Among the reports, angulation of the X-ray beam and rotation of the foot were different, and some of them included fluoroscopic assistance for the adjustment of margins of the tibial plateau. Despite these efforts, none of the radiographic protocols has realized high reproducibility or sensitivity for long-term longitudinal

Table III
Correlations among the KOACAD parameters

	Medial JSA	Lateral JSA	Medial mJSW	Lateral mJSW	Osteopyte area	TFA
Medial JSA	1.00					
Lateral JSA	0.22 (<0.0001)	1.00				
Medial mJSW	0.70 (<0.0001)	0.13 (0.0008)	1.00			
Lateral mJSW	0.18 (<0.0001)	0.72 (<0.0001)	0.22 (<0.0001)	1.00		
Osteophyte area	0.02 (NS)	−0.13 (0.0006)	0.04 (NS)	−0.13 (NS)	1.00	
TFA	−0.08 (0.03)	0.03 (NS)	−0.21 (<0.0001)	−0.19 (<0.0001)	−0.02 (NS)	1.00

Analyses were performed by Pearson's correlation test on 1979 radiographs, and data are expressed as Pearson's correlation values and *P*-values in the parentheses. NS: not significant ($P > 0.05$).

Table IV
Differences of age and the KOACAD parameters between knees with and without pain

	Pain (+)	Pain (−)	*P*-value
Participants (men/women)	594 (124/470)	1385 (575/810)	
Age (years)	76.8 ± 4.7	77.0 ± 4.4	NS
Parameters			
Medial JSA (mm^2)	88.0 ± 1.0	95.7 ± 0.7	<0.0001
Lateral JSA (mm^2)	105.9 ± 1.1	110.2 ± 0.7	0.0013
Medial mJSW (mm)	2.9 ± 1.0	3.3 ± 1.2	<0.0001
Lateral mJSW (mm)	4.3 ± 0.1	4.4 ± 0.0	0.0044
Osteophyte area (mm^2)	4.8 ± 5.4	2.9 ± 7.0	0.0002
TFA (°)	177.9 ± 3.3	176.9 ± 4.3	<0.0001

Analyses were performed on 1979 radiographs, and data are expressed by means ± S.E.M. *P*-values were determined by Student's *t* test. NS: not significant ($P > 0.05$).

studies[27,29]. And, first of all, since these methods increase the cost and require the technician to be specifically trained, they are unlikely to be applicable in general clinical practice or population-based epidemiologic studies. Meanwhile, the conventional standing extended view knee radiographs that the KOACAD system adopted are known to be sensitive to change if the tibial plateau is adequately aligned[30]. To overcome variability of the tibiofemoral joint space by the positioning of the knee and the angulation of the X-ray beam causing the misalignment of the anterior and posterior margins of the tibial plateau, the KOACAD system for the first time designated the middle line between outlines of anterior and posterior margins of the tibial plateau as the lower rim of the radiographic joint space. In fact, reproducibility of all KOACAD parameters was highly maintained with 0° knee flexion and 0–5° X-ray angulation (Table I). This, however, indicates that OA patients with flexion contracture of the knee cannot be appropriately assessed by the KOACAD system, so that patients with more than 5° flexion contracture were excluded from the present study.

Digital images by computed radiographic techniques offer several advantages compared with conventional analog film-screen radiography, and are increasingly available in routine patient management because they allow image enhancement, quantification, archiving, transmission, simultaneous access to the image at multiple sites, and reduction in radiation dose[31]. Although this study used digitized images as the DICOM file, we have confirmed that images digitized from analog radiographs by general image scanners could be used for the KOACAD analysis with perfect reproducibility (ICC = 1.0). In addition, since KOACAD is programmed based on a personal computer, and not on a massive workstation, it can be used anywhere, even away from clinics.

Table V
Multivariate logistic regression analysis for OR and 95% CI of the KOACAD parameters for knee pain

	Men (699)		Women (1280)	
	OR	95% CI	OR	95% CI
Medial mJSW	1.46	1.16–1.90	1.41	1.23–1.63
Lateral mJSW	0.99	0.79–1.23	1.10	0.98–1.24
Osteophyte area	0.99	0.96–1.04	0.99	0.98–1.00
TFA	1.07	1.01–1.13	1.07	1.03–1.10

Data were calculated by stepwise logistic regression analysis after adjustment for age and confounding factors on 1979 radiographs.

The relationship between the radiographic findings and the symptomatic pain in knee joints remains controversial, but at least the severity of radiographic OA is not linearly correlated with that of pain[18–20]. Although the present multivariate analysis was able to detect significant associations of knee pain with low medial mJSW and high TFA, they were not strong (Table V). This may be due to the complicated mechanism underlying the pain. Although articular cartilage is viewed as a major target tissue of OA, knee pain may arise from a number of different structures like joint capsule, ligaments, menisci, bursae, and the bone marrow. Pathological structures caused by OA may contribute to pain indirectly. For example, inflammatory synovitis and associated capillaries are innervated by pain fibers and may be affected in OA[32]. Furthermore, previous MRI surveys among patients with radiographic knee OA showed that knee pain was due not only to OA-related disorders, but also to spontaneous osteonecrosis and bone marrow edema around the knee joint[33–35]. A limitation of the KOACAD system is that these periarticular disorders are not included in the parameters but are best shown by MRI, which might possibly lead to failures in the treatment of knee pain.

Another limitation of this study is a lack of longitudinal investigation to validate the sensitivity of the KOACAD system. One criticism has been that plain radiographs are insensitive to change over time, and that even a small radiographic change is associated with substantial cartilage loss[36]. Nevertheless, the current recommendations suggest that clinical studies of knee OA should include a structural measure of OA severity[5,28]. This emphasizes the need for further refinement in the definition of radiographic outcomes in prospective clinical trials. Recent longitudinal studies using quantitative MRI have shown that subjects with knee OA lose 5% of their tibial cartilage volume per year[37,38] and that the cartilage loss is correlated with worsening of symptoms and portends knee replacement[20,39]. Although the cartilage loss detected by quantitative MRI is much greater than that detected in plain radiographs, the MRI-based cartilage volume correlates with the change of radiographic features to some extent[40,41]. Since the KOACAD system can provide continuous measures of parameters of OA severity, it is possible that the system is as sensitive to change over time as quantitative MRI. Also, the association between knee pain and radiographic features cannot be appropriately assessed in a cross-sectional survey, but should be evaluated over a defined period of time, as indicated by previous reports[42,43]. Our baseline survey in the ROAD study has included quantitative MRI on a group of randomly selected participants. In 2008–2010, we are planning a second survey including the KOACAD radiographic analysis on more than 3000 participants and the quantitative MRI on a portion of these. Comparison of the KOACAD parameters and the MRI findings will validate the sensitivity of the KOACAD system over time, and lead to further understanding of the association between knee pain and radiographic features.

In conclusion, we have established a fully automatic computer-assisted program, KOACAD, to quantify knee OA severity on plain radiographs, and validated its high reproducibility and reliability in a cross-sectional study. This system may not only be useful for objective evaluation of knee OA patients in daily clinical practice or in population-based epidemiologic studies, but also act as a proper surrogate measure for the development of disease-modifying drugs for OA. We hope in the future that this system will be prevalently used worldwide to lead to international criteria for diagnosis and treatment of knee OA, just like BMD in osteoporosis.

Conflict of interest

There are no conflicts of interest.

Acknowledgments

This work was supported by a Grant-in-Aid for Young Scientists from the Japanese Ministry of Education, Culture, Sports, Science and Technology (A18689031), H17-Men-eki-009 from the Ministry of Health, Labor and Welfare, and Research Aid from the Japanese Orthopaedic Association.

Supplementary material

Supplementary material for this article may be found, in the online version, at doi: 10.1016/j.joca.2008.03.011.

References

1. Sharma L, Kapoor D. Epidemiology of osteoarthritis. In: Moskowitz RW, Altman RD, Hochberg MC, Buckwalter JA, Goldberg VM, Eds. Osteoarthritis: Diagnosis and Medical/Surgical Management. 4th edn. Philadelphia: Lippincott Williams & Wilkins; 2007:3–26.
2. Guccione AA, Felson DT, Anderson JJ, Anthony JM, Zhang Y, Wilson PW, *et al.* The effects of specific medical conditions on the functional limitations of elders in the Framingham Study. Am J Public Health 1994;84:351–8.
3. Felson DT, Zhang Y. An update on the epidemiology of knee and hip osteoarthritis with a view to prevention. Arthritis Rheum 1998;41:1343–55.
4. Yelin E, Callahan LF. The economic cost and social and psychological impact of musculoskeletal conditions. National Arthritis Data Work Groups. Arthritis Rheum 1995;38:1351–62.
5. Abadie E, Ethgen D, Avouac B, Bouvenot G, Branco J, Bruyere O, *et al.* Recommendations for the use of new methods to assess the efficacy of disease-modifying drugs in the treatment of osteoarthritis. Osteoarthritis Cartilage 2004;12:263–8.
6. Burstein D, Gray ML. Is MRI fulfilling its promise for molecular imaging of cartilage in arthritis? Osteoarthritis Cartilage 2006;14:1087–90.
7. Eckstein F, Burstein D, Link TM. Quantitative MRI of cartilage and bone: degenerative changes in osteoarthritis. NMR Biomed 2006;19:822–54.
8. Bauer DC, Hunter DJ, Abramson SB, Attur M, Corr M, Felson D, *et al.* Classification of osteoarthritis biomarkers: a proposed approach. Osteoarthritis Cartilage 2006;14:723–7.
9. Kellgren JH, Lawrence JS. Radiological assessment of osteo-arthrosis. Ann Rheum Dis 1957;16:494–502.
10. Altman RD, Hochberg M, Murphy WA Jr, Wolfe F, Lequesne M. Atlas of individual radiographic features in osteoarthritis. Osteoarthritis Cartilage 1995;3(Suppl A):3–70.
11. Altman RD, Gold GE. Atlas of individual radiographic features in osteoarthritis, revised. Osteoarthritis Cartilage 2007;15(Suppl A):A1–A56.
12. Dacre JE, Huskisson EC. The automatic assessment of knee radiographs in osteoarthritis using digital image analysis. Br J Rheumatol 1989;28:506–10.
13. Buckland-Wright JC, Macfarlane DG, Williams SA, Ward RJ. Accuracy and precision of joint space width measurements in standard and macroradiographs of osteoarthritic knees. Ann Rheum Dis 1995;54:872–80.
14. Prakash U, Wigderowitz CA, McGurty DW, Rowley DI. Computerised measurement of tibiofemoral alignment. J Bone Joint Surg Br 2001; 83:819–24.
15. Bruyere O, Henrotin YE, Honore A, Rovati LC, Seidel L, Dardenne C, *et al.* Impact of the joint space width measurement method on the design of knee osteoarthritis studies. Aging Clin Exp Res 2003;15:136–41.
16. Takahashi T, Yamanaka N, Komatsu M, Ogawa Y, Yoshida S, Yamamoto H. A new computer-assisted method for measuring the tibio-femoral angle in patients with osteoarthritis of the knee. Osteoarthritis Cartilage 2004;12:256–9.
17. Linaker CH, Walker-Bone K, Palmer K, Cooper C. Frequency and impact of regional musculoskeletal disorders. Baillieres Clin Rheumatol 1999;13:197–215.
18. Summers MN, Haley WE, Reveille JD, Alarcon GS. Radiographic assessment and psychologic variables as predictors of pain and functional impairment in osteoarthritis of the knee or hip. Arthritis Rheum 1988;31:204–9.
19. Cicuttini FM, Baker J, Hart DJ, Spector TD. Association of pain with radiological changes in different compartments and views of the knee joint. Osteoarthritis Cartilage 1996;4:143–7.
20. Wluka AE, Wolfe R, Stuckey S, Cicuttini FM. How does tibial cartilage volume relate to symptoms in subjects with knee osteoarthritis? Ann Rheum Dis 2004;63:264–8.
21. Boyle RD, Thomas RC. Median filter. In: Boyle RD, Thomas RC, Eds. Computer Vision: a First Course. Blackwell Scientific Publications 1988:32–4.
22. Canny J. A computational approach to edge detection. IEEE Trans Pattern Anal Mach Intell 1986;8:679–714.
23. Hart DJ, Doyle DV, Spector TD. Incidence and risk factors for radiographic knee osteoarthritis in middle-aged women: the Chingford Study. Arthritis Rheum 1999;42:17–24.
24. Jones G, Ding C, Scott F, Glisson M, Cicuttini F. Early radiographic osteoarthritis is associated with substantial changes in cartilage volume and tibial bone surface area in both males and females. Osteoarthritis Cartilage 2004;12:169–74.
25. Kamekura S, Kawasaki Y, Hoshi K, Shimoaka T, Chikuda H. Contribution of runt-related transcription factor 2 to the pathogenesis of osteoarthritis in mice after induction of knee joint instability. Arthritis Rheum 2006;54:2462–70.
26. Yamada T, Kawano H, Koshizuka Y, Fukuda T, Yoshimura K, Kamekura S, *et al.* Carminerin contributes to chondrocyte calcification during endochondral ossification. Nat Med 2006;12:665–70.
27. Brandt KD, Mazzuca SA, Conrozier T, Dacre JE, Peterfy CG, Provvedini D, *et al.* Which is the best radiographic protocol for a clinical trial of a structure modifying drug in patients with knee osteoarthritis? J Rheumatol 2002;29:1308–20.
28. Strand V, Hochberg MC. Study design and outcome measures in osteoarthritis clinical trials. In: Moskowitz RW, Altman RD, Hochberg MC, Buckwalter JA, Goldberg VM, Eds. Osteoarthritis: Diagnosis and Medical/Surgical Management. 4th edn. Philadelphia: Lippincott Williams & Wilkins; 2007:313–25.
29. Mazzuca SA, Brandt KD, Buckwalter KA. Detection of radiographic joint space narrowing in subjects with knee osteoarthritis: longitudinal comparison of the metatarsophalangeal and semiflexed anteroposterior views. Arthritis Rheum 2003;48:385–90.
30. Mazzuca SA, Brandt KD, Dieppe PA, Doherty M, Katz BP, Lane KA. Effect of alignment of the medial tibial plateau and x-ray beam on apparent progression of osteoarthritis in the standing anteroposterior knee radiograph. Arthritis Rheum 2001;44:1786–94.
31. Sanfridsson J, Holje G, Svahn G, Ryd L, Jonsson K. Radiation dose and image information in computed radiography. A phantom study of angle measurements in the weight-bearing knee. Acta Radiol 2000; 41:310–6.
32. Saito T, Koshino T. Distribution of neuropeptides in synovium of the knee with osteoarthritis. Clin Orthop Relat Res 2000;376:172–82.
33. Karachalios T, Zibis A, Papanagiotou P, Karantanas AH, Malizos KN, Roidis N. MR imaging findings in early osteoarthritis of the knee. Eur J Radiol 2004;50:225–30.
34. Felson DT, Chaisson CE, Hill CL, Totterman SM, Gale ME, Skinner KM, *et al.* The association of bone marrow lesions with pain in knee osteoarthritis. Ann Intern Med 2001;134:541–9.
35. Bollet AJ. Edema of the bone marrow can cause pain in osteoarthritis and other diseases of bone and joints. Ann Intern Med 2001;134:591–3.
36. Ravaud P, Giraudeau B, Auleley GR, Drape JL, Rousselin B, Paolozzi L, *et al.* Variability in knee radiographing: implication for definition of radiological progression in medial knee osteoarthritis. Ann Rheum Dis 1998;57:624–9.
37. Wluka AE, Stuckey S, Snaddon J, Cicuttini FM. The determinants of change in tibial cartilage volume in osteoarthritic knees. Arthritis Rheum 2002;46:2065–72.
38. Burgkart R, Glaser C, Hinterwimmer S, Hudelmaier M, Englmeier KH, Reiser M, *et al.* Feasibility of T and Z scores from magnetic resonance imaging data for quantification of cartilage loss in osteoarthritis. Arthritis Rheum 2003;48:2829–35.
39. Cicuttini FM, Jones G, Forbes A, Wluka AE. Rate of cartilage loss at two years predicts subsequent total knee arthroplasty: a prospective study. Ann Rheum Dis 2004;63:1124–7.
40. Raynauld JP, Martel-Pelletier J, Berthiaume MJ, Labonte F, Beaudoin G, de Guise JA, *et al.* Quantitative magnetic resonance imaging evaluation of knee osteoarthritis progression over two years and correlation with clinical symptoms and radiologic changes. Arthritis Rheum 2004;50:476–87.
41. Cicuttini F, Hankin J, Jones G, Wluka A. Comparison of conventional standing knee radiographs and magnetic resonance imaging in assessing progression of tibiofemoral joint osteoarthritis. Osteoarthritis Cartilage 2005;13:722–7.
42. Ledingham J, Regan M, Jones A, Doherty M. Factors affecting radiographic progression of knee osteoarthritis. Ann Rheum Dis 1995;54: 53–8.
43. van Dijk GM, Dekker J, Veenhof C, van den Ende CH. Course of functional status and pain in osteoarthritis of the hip or knee: a systematic review of the literature. Arthritis Rheum 2006;55:779–85.

Transactions of the Materials Research Society of Japan 33[3] 771-774 (2008)

Nanoscale Structured Phospholipid Polymer Brush for Biointerface

Kazuhiko Kitano[1], Ryosuke Matsuno[2,3], Tomohiro Konno[2,3],
Madoka Takai[2,3], and Kazuhiko Ishihara[1,2,3]
[1]Department of Bioengineering, [2]Department of Materials Engineering, [3]Center for NanoBio Integration (CNBI),
The University of Tokyo, 7-3-1, Hongo, Bunkyo-ku, Tokyo 113-8656, Japan,
Fax: +81-3-5841-8647, e-mail: kitano@mpc.t.u-tokyo.ac.jp

To prepare the biomaterial surface having both lubricity and biocompatibility, we aimed to prove the mechanism of the resistance of friction and protein adsorption with grafting polymer. We prepared poly(2-methacryloyloxyethyl phosphorylcholine) (PMPC) grafted layer using an atom transfer radical polymerization (ATRP) method, which had the advantage of controlling surface structures on nanoscale. From the results of surface characterization, it was confirmed that the thickness of the PMPC grafted layer was 4-10 nm and the conformation of the PMPC grafted layer was brushlike. We investigated the friction properties in air and in water with an atomic force microscopy (AFM). The friction coefficients of the PMPC brush layers were decreased dramatically in water and the resistance of friction depended on the thickness of the PMPC brush layer. We also investigated the protein adhesion properties by measuring the force-distance curves using the AFM cantilever immobilized with a bovine serum albumin (BSA). The adhesion force between the BSA and the PMPC brush layers were markedly reduced and the resistance of the BSA adhesion depended on the thickness of the PMPC brush layer. For resisting both friction and protein adsorption in water, it was a key factor to keep the thick hydrated layer made by the elongated hydrophilic PMPC brush chains.
Key words: phospholipid polymer, polymer brush, atom transfer radical polymerization, atomic force microscopy, lubricity

1. INTRODUCTION

In recent years there has been increasing interest in surface modification with polymers to improve a solid surface properties for biomaterials. Lubricity is one of the essential properties for biomaterials such as artificial joints, blood pump bearings, and catheters. As for artificial joints, the loosening caused by wear between the articulating surfaces is the most serious problem limiting their survival and clinical success. We aimed for obtaining both lubricity and biocompatibility for biomaterial surfaces. We used poly(2-methacryloyloxyethyl phosphorylcholine) (PMPC) as a surface modifier, which is well known for biocompatible polymer whose side chain is composed of phosphorylcholine resembling phospholipid of cell membrane[1-4]. The polymers with MPC units onto the surface of medical devices have already been shown to suppress biological reactions when they are in contact with living organisms. Using the fundamental research results, PMPC are now clinically used on the surfaces of intravascular stents, guide wires, soft contact lenses, and artificial heart[5-7]. Surface grafting of PMPC is excellent method to obtain the biocompatibility[8-10]. We expect that the PMPC grafting also improves lubricity of a solid surface because there are the same phospholipid polar groups on the surface of the human articular cartilage. It has been reported that the PMPC grafting onto the polyethylene liner of the artificial hip joint clearly reduced wear between the articulating surfaces for long term[11,12]. However why the PMPC grafting improves surface lubricity or biocompatibility has not been clear yet. In this study, in order to investigate the surface properties of the PMPC grafted surface, we prepared the nanoscale structured PMPC grafted layer using an atom transfer radical polymerization (ATRP) method, which was famous for preparing well-controlled polymer grafted layer[13,14]. We mainly studied two surface properties on nanoscale. The first is about the friction properties. We measured the friction force of the PMPC grafted surfaces with an atomic force microscopy (AFM). The second is about the protein adhesion properties. We obtained force-distance (*f-d*) curves with a protein immobilized AFM cantilever, and calculated adhesion force of the protein on the PMPC grafted surfaces.

2. EXPERIMENTS

2.1 Surface preparation

2.1.1 Surface-initiator immobilization

SiO_2 coated silicon wafers (Si) were cut into 1.0 cm x 2.0 cm, rinsed sufficiently with acetone and ethanol and treated with oxygen plasma. To prepare the homogeneous monolayer of the initiator on the silicon wafers, monochlorosilane, 3-(2-bromoisobutyryl)-propyl dimethylchlorosilane (BDCS), was used as the surface initiator. We synthesized BDCS as previously described[15]. The cleaned substrates were immersed in a 5 mmol/L toluene solution of BDCS for 24 h. The wafers were removed from the solution, rinsed with methanol, and dried in an argon stream before used for the graft polymerization.

2.2.2 Graft polymerization of MPC

The graft polymerization of MPC on the silicon wafers was performed using an ATRP method. MPC was dissolved in 10mL of dehydrated methanol. Copper bromide (I) (20 mg, 0.135 mmol) and 2,2'-dipyridyl (43 mg, 0.27 mmol) were added with stirring under argon at room temperature. The amount of MPC was changed

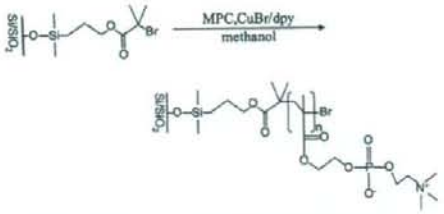

Fig.1 Preparation of the PMPC brush layers on silicon wafer via ATRP.

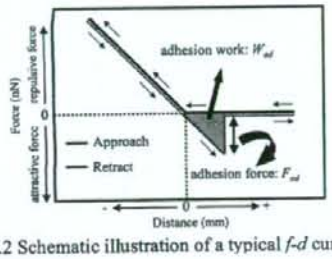

Fig.2 Schematic illustration of a typical *f-d* curve.

variedly in order to control the thickness of the PMPC brush layers. After the solution was stirred for 30 min under an argon gas atmosphere, the BDCS immobilized silicon wafers were immersed into the solution and at the same time ethyl 2-bromoisobutyrate (20 μL, 0.135 mmol) was added as a sacrificial initiator. The polymerization was carried out at room temperature with stirring under an argon gas atmosphere. The silicon wafers were removed from the polymerization mixture after the desired time period. Subsequently, they were extracted with a Soxleht apparatus in methanol for 20h and dried in vacuo at room temperature. The scheme of the reaction is shown in Fig.1.

2.3 Surface characterization

The surface chemical composition was determined by X-ray photoelectron spectroscopy (XPS). Survey scans (0-1100 eV) were performed to identify the C, N, O, and P elements. A take off angle of the photoelectrons was 90°. All binding energies were referenced the C_{1s} peak at 285 eV. The static water contact angles were measured using a goniometer at room temperature. Water droplets of 6 μL were contacted onto the substrates and the contact angles at 10 sec were directly measured by photographic images. The data was collected at 3 positions on each sample. The thickness of the PMPC brush layers in air was measured by ellipsometry. The surface morphology of the PMPC brush layers was observed with an AFM in air. Images were captured in a 1 μm x 1 μm area.

2.4 Interfacial friction measurements

A Nanoscope IIIa AFM (Digital Instruments) was used to characterize interfacial friction properties. Experiments were performed in contact mode in air and in water. V-shaped Si_3N_4 cantilevers with an announced force contact of 0.12 N/m were used. Surface friction data were acquired by scanning in the Trace and Retrace directions by disabling the slow scan axis. The friction voltage signals were corrected and converted to units of force by the previously proposed method[16]. For investigating the friction-load relationship, the scan size was maintained at 2.0 μm and the scan rate at 2.0 Hz, giving a sliding velocity of 8 μm/s. The applied load was varied by changing the vertical deflection of the cantilever. The load was calculated with a method reported previously.[17]. To calculate the load, we measured the *f-d* curve right after every friction imaging. The friction versus sliding velocity measurements was carried out between the sliding velocity of 0.4 μm/s and 488 μm/s. A scan size of 2 μm was used for the measurements.

2.5 Investigation of the protein adhesion properties

2.5.1 Bovine serum albumin (BSA) immobilization onto the AFM cantilever

The BSA-immobilized cantilever was prepared as follows. The oxygen-plasma treated Si_3N_4 cantilever was reacted with an ethanol solution of 3-aminopropyltriethoxysilane (APTES) for 2 h at room temperature, and then rinsed with water and ethanol. The surface silanized with APTES was reacted with a 5 % solution of glutaraldehyde in phosphate buffered saline (PBS) for 3 h, and then rinsed with PBS, followed by immersing in 3 mg/mL BSA in PBS at 37 °C for 3 h. The cantilever was then rinsed with PBS.

2.5.2 Measurements of the *f-d* curves

We measured the *f-d* curves in PBS (pH = 7.4) using the BSA-immobilized AFM cantilever and obtained the adhesion properties between the BSA and the PMPC brush layers. Fig.2 shows a typical *f-d* curve for an AFM cantilever contacted with a solid surface. The maximum normal deflection of the retracting curve was defined as adhesion force, F_{ad}, and the area framed by approaching curve and retracting curve was defined as adhesion work, W_{ad}. We used these two parameters for comparing adhesion properties. More than two *f-d* curves were obtained at one location through repeated cantilever approach/retract cycles, and the measurements were also repeated at more than five locations on each sample.

3. RESULTS AND DISUCUSSIONS

3.1 Surface characterization

The grafting of PMPC on the silicon wafers was confirmed using XPS. The peaks in the carbon atom region (C_{1s}) at 286 eV and 289 eV indicated the ether bond and the ester bond, respectively, and those in the nitrogen atom region (N_{1s}) at 403 eV and phosphorus atom region (P_{2p}) at 133 eV were specific to the phosphorylcholine group in the MPC unit. The results of the contact angle and the dry thickness are shown in Fig.3. The static water contact angles on the PMPC brush layers were about 10-25°, which was 20-30 % of those on the unmodified Si. The PMPC grafting greatly increased hydrophilicity, and a very little introduction of the PMPC chains made dramatic effects on the wettability by water. The thickness of the PMPC brush layers was increased with an increase in polymerization degree. We controlled the thickness of the PMPC brush layers by changing the amount of the MPC monomer in the polymerization solution. The dry thickness of the PMPC brush layers was used to estimate the graft density σ by,

$$\sigma = h\rho N_A / M_n$$

where h is the layer thickness determined by ellipsometry, ρ is the density of dry polymer layer

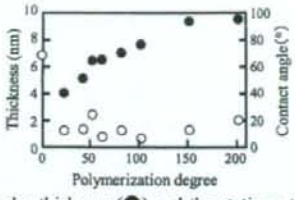

Fig.3 The dry thickness (●) and the static water contact angle (○) of the PMPC brush layers.

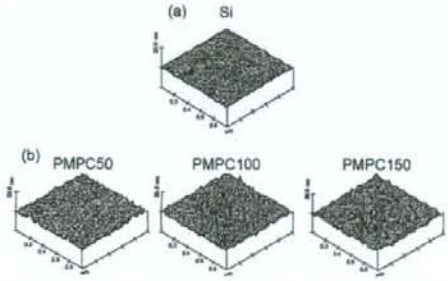

Fig.4 The AFM images of (a) the unmodified Si, (b) PMPC 50, PMPC 100, and PMPC 150.

(1.30g/cm^3 for PMPC[13]), N_A is Avogadro's number, and M_n is the number-average molecular weight of a polymer chain grafted on surface. M_n was determined by measuring the molecular weight of a free polymer because previous reports described that the molecular weight of a polymer chain grafted on surface was the same as that of a free polymer[18]. As a result, the average of the graft density of the PMPC brush layers was 0.17 chains/nm^2. It was said that polymer-grafted layer which had more than 0.10 chains/nm^2 graft density became high dense brush conformation[19]. We confirmed that the PMPC grafted layer prepared via ATRP became "brush" layer. We also confirmed the brush conformation of the PMPC grafted layers with an AFM in dry condition. The AFM images are shown in Fig.4. Compared with the unmodified Si, brush structure of the PMPC 50, 100, and 150 (the numbers, 50, 100, and 150, were the polymerization degree) was observed. The root-mean-square (RMS) surface roughness of all samples was about 0.5 nm, which indicated that the PMPC brush layers prepared by ATRP were very homogeneous.

3.2 Friction properties

Interfacial friction forces for the unmodified Si, PMPC 50, PMPC 100, and PMPC 150 measured as a function of normal load in air (a) and in water (b) are shown in Fig.5. In air, the friction coefficients of the PMPC brush layers were the same value as those of the unmodified Si, and showed the same behavior, which characteristically showed the high friction coefficients under lower load. These results were due to the adhesion force between the AFM cantilever and the substrate acting as normal load. The adhesion force between the AFM cantilever and the unmodified Si was 10-30 nN, measured by the *f-d* curves. Under lower load, the adhesion force had relatively a large effect on normal load and the friction coefficients became very high. The same value of the adhesion force was measured by the *f-d* curve measurements about the PMPC brush layers in

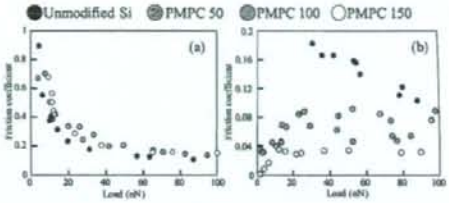

Fig.5 The friction coefficients as a function of normal load in (a) air and in (b) water.

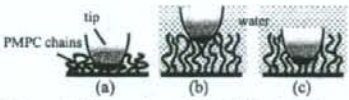

Fig.6 Schematic illustration of the sliding interface (a) in air, (b) in water under lower load, and (c) in water under higher load.

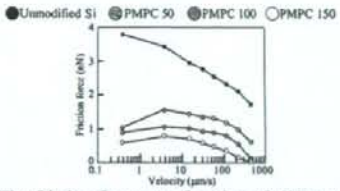

Fig.7 The friction force as a function of sliding velocity in water.

air. It was indicated that the PMPC chains were compressed in air and had no effect on interaction between the AFM cantilever and the silicon substrate (Fig.6 (a)). On the other hand, in water, the friction coefficients of the PMPC brush layers greatly decreased. Under lower load, the friction coefficients of the PMPC brush layers were especially low, and gently increased as normal load increased. These results indicated that the adhesion force between the AFM cantilever and the substrate did not occur on the PMPC brush layers in water because the hydrophilic PMPC chains elongated in water, took in a lot of water, and made the hydrated layer (Fig.6 (b)). The PMPC hydrated layer prevented from the direct contact between the AFM cantilever and the substrate, and achieved highly lubricity. As normal load increased, the AFM cantilever penetrated into the layer (Fig.6 (c)), and the interaction against the substrate gradually occurred. This was the reason why the friction coefficients increased as normal load increased. Seen from the thickness dependency, the friction coefficients of the PMPC brush layers decreased with an increase in the thickness of the PMPC brush layer because the thicker brush layer made the thicker hydrated layer. Satisfying the condition of noncontact friction interfaces leads to very low friction.

The friction forces measured as a function of a sliding velocity in water are shown Fig.7. The friction force of the unmodified Si decreased monotonically with an increase in the sliding velocity. On the other hand, there was maximum value in the friction force-velocity curve about the PMPC brush layers. These phenomena were also found in gel friction reported by Gong *et al.*[20]. By

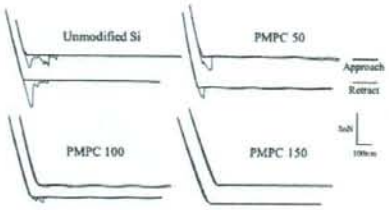

Fig.8 The representative *f-d* curves measured with the BSA- immobilized cantilever.

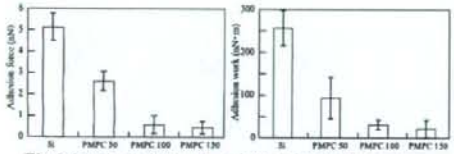

Fig.9 (a) F_{ad} and (b) W_{ad} calculated with *f-d* curves.

reference to this report, the reason for these results was that the elastic deformation of the PMPC brush chains was measured as the friction force under the low sliding velocity. When the sliding velocity became higher than the elastic mobility of the PMPC brush chains, the elastic deformation did not contribute to the friction force and the friction decreased with an increase in the sliding velocity.

3.3 Protein adhesion properties

The representative *f-d* curves measured with the BSA immobilized cantilever are shown in Fig.8, and F_{ad} and W_{ad} are shown in Fig.9. It was confirmed that the adhesion force between the BSA and the PMPC brush layers was markedly reduced and then decreased with an increase in the thickness of the PMPC brush layers. The F_{ad} and W_{ad} of PMPC 150 was nearly measurement limit, so it was believed that PMPC 150 had little or no interaction with BSA. Hydrophobic interaction is a main interaction when a protein adheres a solid surface, reported by Kidoaki *et al.*[21]. The hydrophilic PMPC brush layers resisted hydrophobic interaction with the BSA. In addition to the reduction of hydrophobic interaction, hydration repulsive force caused the resistance of the BSA adhesion force. Hydration repulsive force said to be a short-range force that usually appeared at nanoscale separation distances and arose whenever water molecules bind to strongly hydrophilic materials. Therefore, the required properties for resisting the protein adhesion are not only just hydrophilicity but also the ability to couple many water molecules, which means that making the thick hydrated layer. The thickness of the hydrated layer increased as the thickness of the polymer brush layer increased, considered from the friction measurements. Hydration repulsive force is the reason why the resistance of the BSA adhesion force depended on the thickness of the polymer brush layer.

4. CONCLUSIONS

We prepared the well-controlled PMPC brush layer using an ATRP method. We controlled the thickness of the PMPC brush layers on nanoscale by changing the amount of the MPC monomer in the polymerization solution. From the nanoscale friction measurements by AFM, it was most important for obtaining lubricity to satisfy the condition of noncontact friction interfaces with the hydrated layer. From the *f-d* curves measurements using the BSA-immobilized cantilever, the BSA adhesion force was clearly decreased by the PMPC grafting because of both the reduction of hydrophobic interaction and the increase of hydration repulsive force. The hydrated layer made by the elongated PMPC brush layer in water served a key role in leading to excellent lubricity and biocompatibility.

Acknowledgement

A part of this research was supported by the Core Research for Evolution Science and Technology (CREST) from Japan Science and Technology Agency (JST).

References

[1] K. Ishihara, T.Ueda, and N.Nakabayashi, *Polym.J.*, 32, 355-360 (1990)
[2] K. Ishihara, N. P. Ziats, B. P. Tierney, N. Nakabayashi, and J. M. Anderson, *J. Bone Miner. Res.*, 25, 1397-1407 (1991)
[3] K. Ishihara, H. Oshida, T. Ueda, Y. Endo, A. Watanabe, and N. Nakabayashi, *J. Bone Miner. Res.*, 26, 1543-1552 (1992)
[4] P. C. Chang, S. Lee, and G. Hsiue, *J. Bone Miner. Res.*, 39, 380-389
[5] T. A. Snyder, H. Tsukui, S. Kihara, T. Akimoto, K. N. Litwak, M. V. Kameneva, K. Yamazaki, and W. R. Wagner, *J. Biomed. Mater. Res. A*, 81, 85-92 (2007)
[6] S. Sawada, Y. Iwasaki, N. Nakabayashi, and K. Ishihara, *J. Biomed. Mater. Res. A*, 79, 476-484 (2006)
[7] A. L. Lweis, L. A. Tolhurst, and P. W. Startford, *Biomaterials*, 23, 1697-1706 (2002)
[8] J. Sibarani, M. Takai, and K. Ishihara, *Colloids and Surf. B*, 54, 88-93 (2007)
[9] T. Goda, R. Matsuno, T. Konno, M. Takai, and K. Ishihara, *Colloids and Surf. B*, in Press (2007)
[10] W. Feng, S. Zhu, K. Ishihara, and J. L. Brash, *Langmuir*, 21, 5980-5987 (2005)
[11] T. Moro, Y. Takatori, K. Ishihara, T. Konno, Y. Takigawa, T. Matsushita, U. Chung, K. Nakamura, and H. Kawaguchi, *Nature Materials*, 3, 829-835 (2004)
[12] M. Kyomoto, T. Moro, T. Konno, H. Takadama, N. Yamawaki, H. Kawaguchi, Y. Takatori, K. Nakamura, and K. Ishihara, *J Biomed Mater Res Part A*, 82, 10-17 (2007)
[13] R. Iwata, P. Suk-In, V. P. Hoven, A. Takahara, K. Akiyoshi, and Y. Iwasaki, *Biomacromolecules*, 5, 2308-2314 (2004)
[14] M. Kobayashi, N. Hosaka, M. Kaido, A. Suzuki, N. Yamada, N. Torikai, K. Ishihara, and A. Takahara, *Soft Matter*, 3, 1-8 (2007)
[15] A. Ramakrishman, R. Dhamodharan, and J. Ruhe, *Macromol Rapid Commun*, 23, 612-616 (2002)
[16] Y. Liu, and D. F. Evans, *Langmuir*, 12, 1235-1244 (1996)
[17] J. Li, C. Wang, G. Shang, Q. Xu, Z. Lin, J. Guan, and C. Bai, *Langmuir*, 15, 7662-7669 (1999)
[18] M. Husseman, E. E. Malmstrom, M. McNamara, M. Mate, D. Mecerreyes, D. G. Benoit, *Macromolecules*, 32, 1424-1431 (1999)
[19] Y. Tsujii, K, Ohno, S. Yamamoto, A. Goto, T. Fukuda, *Adv Polym Sci*, 197, 1-45 (2006)
[20] J. P. Gong, Y. Osada, *J Chem Phys*, 109, 8062 (1998)
[21] S. Kidoaki, T. Matsuda, *Langmuir*, 15, 7639-7646 (1999)

(Recieved December 9, 2007 ; Accepted April 5, 2008)

Journal of Orthopaedic Nursing (2008) 12, 75–83

ELSEVIER

Journal of Orthopaedic Nursing

www.elsevier.com/joon

A study of disease management activities of hip osteoarthritis patients under conservative treatment

Yurie Koyama RN (PhD) [a,c,*], Mitsunori Miyashita RN, M.HLTH.SC (PhD) [a], Shinji Irie RN [a], Motoi Yamamoto MD [b], Tatsuro Karita MD [b], Toru Moro MD [b], Yoshio Takatori MD [b], Keiko Kazuma RN (PhD) [a]

[a] *Department of Adult Nursing/Palliative Care Nursing, School of Health Sciences and Nursing, Graduate School of Medicine, The University of Tokyo, 7-3-1 Hongo, Bunkyo-ku, Tokyo, Japan*
[b] *Department of Orthopaedic Surgery, Graduate School of Medicine, The University of Tokyo, Tokyo, Japan*
[c] *The National College of Nursing, 1-2-1, Umezono, Kiyose-shi, Tokyo, Japan*

KEYWORDS
Disease management;
Hip osteoarthritis;
Conservative treatment

Summary The study aimed to determine the status of disease management activities that patients under conservative treatment actually performed and to examine the relevant factors in performing or not performing the activities. A survey was conducted with hip OA patients of the orthopaedic outpatient service of one university hospital in Japan. Results indicated that it is necessary to advise patients at an earlier stage of the disease to perform the management activities and to develop a program to link the advice to actual performance of the activities.

Editor's comments
Mobility and mobilising patients are the essence of orthopaedics. This study provides a fascinating and much needed insight into the approach we should adopt when using conservative treatments for osteoarthritis of the hip even though many patients go on to have the almost inevitable surgery. **PD**

Introduction

Hip osteoarthritis (OA) is a progressive chronic disease with pain and restricted range of motion, causing disorder in activities in daily life (ADL). In Japan, secondary disease of the hip joint resulting from dysplastic hip is common. In most cases, patients have symptoms such as pain or discomfort in their 1920s and 1930s and are diagnosed as having hip

* Corresponding author. Department of Adult Nursing/Palliative Care Nursing, School of Health Sciences and Nursing, Graduate School of Medicine, The University of Tokyo, 7-3-1 Hongo, Bunkyo-ku, Tokyo, Japan. Tel.: +81 3 5841 3508; fax: +81 3 5841 3502.
E-mail address: koyamayu-tky@umin.ac.jp (Y. Koyama).

1361-3111/$ - see front matter
doi:10.1016/j.joon.2008.07.005

disease. Gradual degeneration over time is a characteristic of the disease, and in the slow progression of the symptoms, pain and restriction in the range of motion gradually increase over 10–30 years. If congruency in not acceptable, osteotomy is performed to prevent further development of OA (Honda et al., 1999). However, a limited number of patients can have surgery because of the indication required for arthroplasty, such as joint compatibility and the rate of progression. Typical surgery, total hip replacement (THR), is performed in Japan for OA patients aged 60 or over who have disorders in ADL due to unrelieved pain (Creamer et al., 1998; Anon., 2000; Dolin et al., 2003). Therefore, conservative treatment is the first line in treatment of OA. Patients are required to find a way of controlling their pain and managing the disease, by doing weight management and muscle training in daily life (Anon., 2000; Manek and Lane, 2000).

In conservative treatment, weight reduction and muscle training are firstly recommended. Weight reduction is important to reduce the load on the hip joint (Arokoski, 2005). The hip joint is subjected to a load three times that of the body weight (Davy et al., 1988) and patients are directed not to lift heavy objects or remain standing for long periods. A large randomized clinical trial (RCT) (van Baar et al., 1998) verified that weight reduction and muscle training lead to pain relief and improvement in the range of motion of the hip. The guideline suggests that exercises, including stretching and muscle training, have an effect of slowing the progress of the disease (Hochberg et al., 1995; Anon., 2000). Doctors explain this importance to patients and advise them to accept and practice the therapy in their daily lives.

However, in contrast to those who have surgery, patients having conservative treatment regimes usually visit the university hospital only about once a year and have few opportunities for medical guidance and information provision. If the disease becomes worse, and patients cannot relieve their pain even though muscle training is performed aggressively, doctors may suggest total hip replacement. Doctors give most patients the instruction of muscle training, mainly strengthening the adductors by lifting each leg in a recumbent position. Additionally, individual training can be provided whenever they request. Disease management is controlled by the patients themselves.

Methods

The survey was conducted with OA patients of the orthopaedic outpatient service of one university hospital who agreed in writing to participate in the study and satisfied the following conditions:

- Had not undergone a joint-preserving procedure or THA.
- Receiving conservative treatment using a cane and drugs such as NSAIDs and physical therapy – including exercises and stretch exercises.
- Were between the ages of 20 and 80 at the time of survey.
- Could communicate in Japanese.
- Had no dementia and could fill in the questionnaire sheet.

Patients were asked through doctors to cooperate in the research. Our staff explained the aim of the survey to the patients in a private room and received their letters of consent. Staff gave the patients the questionnaire to fill in by themselves in the room and collected the questionnaire directly from the patients. Their current Japanese Orthopaedics Association (JOA) score and number of years of being a patient were extracted from medical records, and the height and weight of the patients were measured. The survey was conducted from August 2003 to August 2004.

The questionnaire presented nine statements regarding disease management activity:

1. I try not to remain standing for long periods of time.
2. I do not choose shoes with high heels or hard soles.
3. I am careful about the walking distance and speed in daily life.
4. I use a cane or hold a handrail when necessary.
5. I try not to lift heavy objects.
6. I do muscle training.
7. I am careful with my diet to avoid weight gain.
8. I do stretching.
9. I do exercise to prevent weight gain.

The subjects answered Yes or No to these statements.

Other factors relevant to the disease management activity, such as age, number of years of being a patient, body mass index (BMI), JOA score, and discomfort in daily life were also studied. ''Discomfort in daily life'' was investigated by asking patients about what they felt was difficult in their daily life using answers graded from 1 to 5. The questions were:

1. There are no local medical specialists for disease management.
2. I find it difficult to maintain my body weight appropriately.

3. I have a hard time controlling pain in daily life.
4. I am reluctant to use a walking stick.
5. I have a hard time moving joints as I wish.
6. It is difficult to choose a treatment method.
7. I feel that I am putting burdens on my family or friends.
8. I have a hard time sleeping well due to pain.

These eight statements were created by researchers based on the result of preliminary interviews with 24 OA patients of the orthopaedic outpatient service and on earlier studies. Then necessary revision was made to the statements according to the examination of face validity based on the opinions of five medical specialists and five nurses who had more than 3 years experience in orthopedics. To examine the effectiveness of the survey sheets, a preliminary survey was conducted for eight patients, and necessary revision was made on the questions for the main survey.

Sex, age, disease stage, and number of years of being an OA patient were extracted from medical records. Occupation if any, financial status, and academic background were asked about on the survey sheet.

We analyzed the disease stage by dividing it into four stages: pre OA, primary stage, advanced stage, and end stage. If a patient had hip OA on both sides, the stage and JOA score on the more advanced side were used.

The ratio of the answers to the statements on the disease management activities was calculated for each disease stage. We used Mantel-Haenszel's chi-square test to examine any tendency in the fraction of the activities at each stage. A *t-test* was used for differences between one-side hip OA and two-side hip OA of disease management activities. We performed factor analysis on the nine statements of the disease management activities using the principal factor method with Promax Rotation, and calculated the coefficients of the correlation between the total score of the domain, derived from the factor analysis, and related factors. We performed a two-sided test with 5% significant level, using SAS Windows edition Version 9.1.

The Ethical Committee of the Faculty of Medicine, the University of Tokyo, approved the study. We explained the details of the study to the patients using a briefing document. They could stop participating in the study whenever they wished, as we thus tried not to force them to agree to the participation, and assured them that subsequent medical treatment would not be affected even if they refused or stopped the participation. We explained all of these factors to the patients and conducted the research for those patients who provided written consent to participate in the study.

Results

The questionnaire was distributed to 339 patients and the completed questionnaire was collected from 330 patients (response rate of 97%). Those who did not agree to cooperate gave their reasons for disagreement: 7 patients answered that they did not have enough time, 1 answered that he/she felt bad, and 1 answered that he/she did not understand the purpose of the research.

Table 1 shows the characteristics of all the patients and of the patients at each disease stage. The average age of the patients was 51 years (SD13). Females occupied 89% and the BMI was 23 (SD 3). The average period of being a patient was 7 years (SD 3), and the JOA score was 68 points (SD 20).

Table 2 shows the achievement ratio of the management activities. More than 85% of the patients answered yes to the statement "I try not to remain standing for long periods of time." and "I do not choose shoes with high heels or hard soles." Seventy-three percent of patients answered yes to the statements "I do muscle training." and "I am careful with my diet to avoid weight gain." The patients at the advanced stage tended to answer yes to these statements. To the statements "I do stretching." and "I do exercise to prevent weight gain," more than half of all the patients, and less than half of the patients answered no.

Differences between one-side hip OA and two-side hip OA of disease management activities are shown in Table 3. Results of a *t-test* showed no significant differences between two groups.

About 70% of the patients answered that they performed the disease management activities because "I do not want to let OA progress" or "I want to control pain." About 50% gave the reason that "I do not want to have surgery." About 20% answered that "I was told by doctors to do so" (Table 4).

We show in Table 5 the result of the factor analysis to examine the pattern of the nine disease management activities. As a consequence, we extracted ⟨muscle training and weight management activities⟩ as the first factor, ⟨Activities to prevent load on hip⟩ as the second, and ⟨Activities to aid careful walking⟩ as the third. The factor loading of "I am careful with my diet to avoid weight gain" was relatively low, 0.3, but we included it in the first factor ⟨Positive management activities⟩ from the clinical perspective. Cronbach's α coefficient of each factor was in the

Table 1 Background of the patients

		Total		Pre OA		Primary		Progressive		End	
		N = 330		*n* = 56		*n* = 49		*n* = 68		*n* = 157	
Age (years)	Mean (SD)	51	(13)	38	(10)	44	(12)	50	(10)	59	(9)
Sex (Female)	%	89%		91%		90%		91%		88%	
Weight (kg)	Mean (SD)	55	(9)	54	(8)	55	(8)	57	(9)	54	(9)
BMI[a] (kg/m^2)	Mean (SD)	23	(3)	22	(3)	22	(3)	23	(3)	23	(3)
Duration of osteoarthritis (years)	Mean (SD)	7	(7)	6	(5)	7	(7)	6	(7)	9	(8)
Academic background (high school graduate or below)	%	44%		25%		24%		35%		60%	
Economic condition (the better)[a]	%	12%		13%		18%		7%		13%	
Job-having	%	48%		66%		47%		59%		37%	
JOA score[b]	Mean (SD)	68	(20)	88	(10)	81	(13)	71	(15)	56	(17)
Range of motion	Mean (SD)	13	(6)	19	(2)	18	(2)	15	(3)	9	(5)
Pain	Mean (SD)	26	(10)	31	(7)	28	(8)	25	(9)	23	(11)
Ability to walk	Mean (SD)	14	(5)	18	(3)	17	(3)	14	(4)	11	(5)
Activity of daily life	Mean (SD)	16	(4)	19	(2)	18	(3)	16	(3)	13	(3)
Difficulty in their daily life[c]											
There are no local medical specialists for disease management	%	20%		5%		22%		10%		29%	
I find it difficult to maintain my body weight appropriately	%	45%		41%		43%		46%		47%	
I have a hard time controlling pain in daily life	%	23%		16%		10%		24%		30%	
I am reluctant to use a walking stick	%	43%		36%		43%		44%		46%	
I have a hard time moving joints as I wish	%	49%		13%		31%		51%		68%	
It difficulty to choose a treatment method	%	41%		27%		39%		41%		46%	
I feel that I am putting burdens on my family or friends	%	42%		27%		31%		41%		52%	
I have a hard the sleeping well due to pain	%	19%		9%		8%		18%		27%	

[a] BMI: Body Mass Index.
[b] JOA score (In the bi-lateral hip OA group, the score of the more advanced hip joint was adopted).
[c] The numbers in the table show the rate of responses for "I live in fairly affluent circumstances." and "I live in very affluent circumstances".